
C. T. YERKES
M. S.

This is to certify that the

thesis entitled

THE KINETICS OF ELECTRON TRANSFER REACTIONS IN CHLOROPLAST PHOTOSYSTEM II

presented by

Christine Thompson Yerkes

has been accepted towards fulfillment
of the requirements for

M.S. degree in Chemistry

G. T. Babcock
Major professor

Date 2/21/79

THE KINETICS OF ELECTRON TRANSFER REACTIONS IN CHLOROPLAST PHOTOSYSTEM II

By

Christine Thompson Yerkes

A THESIS

Submitted to
Michigan State University
in partial fulfillment of the requirements
for the degree of

MASTER OF SCIENCE

Department of Chemistry

1979

ABSTRACT

THE KINETICS OF ELECTRON TRANSFER REACTIONS IN CHLOROPLAST PHOTOSYSTEM II

By

Christine Thompson Yerkes

The rate of photosynthetic oxygen evolution, measured polarographically under conditions of continuous illumination, is examined as a function of pH in the presence of a variety of uncoupling agents. A pH optimum is observed at about pH = 7.0 for all cases. A model has been developed and tested to explain the uncoupler mode of action and the complicating role of the membrane.

To define the origin of the observed pH dependence of oxygen evolution, analogous experiments have been carried out using the EPR detectable species, signal II_f, as a probe for the electron transfer kinetics on the water side of Photosystem II, the site of oxygen evolution. A model has been developed to explain the pH dependence of signal II_f decay kinetics in the presence of ascorbate. The kinetic model shows good agreement with the experimental data if either a pH dependent proton gradient across the membrane or a negative interior surface charge is postulated.

ACKNOWLEDGEMENTS

I would like to thank Martin Rabb for his technical assistance, the staff of the electronics shop for their patience and especially Professor Jerry Babcock for his guidance in this project. Its existence attests to the fact that his enthusiasm and scientific curiosity finally proved contagious.

TABLE OF CONTENTS

LIST OF TABLES

LIST OF FIGURES

ABBREVIATIONS

ADP	Adenosine diphosphate
ATP	Adenosine triphosphate
Asc^-	Ascorbate
Chl	Chlorophyll
Cyt	Cytochrome
EDTA	Ethylenediaminetetraacetic acid
EMF	Electromotive force
EPR	Electron Paramagnetic Resonance
Fd	Ferredoxin
HAsc	Ascorbic acid
HEPES	N-2-Hydroxyethylpiperazine-N'-2-ethanosulfonic acid
HQ	Hydroquinone
MES	2(N-morphalino)ethanesulfonic acid
NADP	Nicotinamide adenine dinucleotide phosphate
NADPH	Nictoinamide adenine dinucleotide phosphate, reduced form
P_i	Inorganic phosphorous
PCy	Plastocyanin
PQ	Plastoquinone
PS I	Photosystem I
PS II	Photosystem II
TRICINE	N-tris(hydroxymethyl)methylglycine
TRIS	Tris(hydroxymethyl)aminomethane
X	Magnetic susceptibility

INTRODUCTION

Although many advances have been made in understanding the photosynthetic process in bacteria and higher organisms, the photosynthetic evolution of oxygen remains a major process whose mechanism has not been explained. The role of oxygen evolution relative to the other light driven reactions in photosynthesis is described in Figure 1, a schematic representation of the overall process of higher plant photosynthesis. This model, often referred to as the Z scheme, can be conveniently divided into two photochemical systems: Photosystem I (PS I) associated with the reduction of NADP and Photosystem II (PS II) associated with the oxidation of water. The light harvesting components, referred to as antenna pigments, are capable of transferring energy via both exciton interaction and Forster transfer (Sauer, 1978) to specialized molecules called reaction centers. These two forms of chlorophyll, antenna pigments and reaction centers, exist in a ratio of about 400 to 1 (Emerson and Arnold, 1932). Light energy absorbed by the light harvesting system of PS II is trapped at a reaction center called P680. The name of this component is derived from its presumed absorption maximum at 680 nm. Light induced charge separation at this reaction center leads to the reduction

Figure 1. The basic elements of the Z-scheme, two light reaction hypothesis for green plant photosynthesis. Vertical arrows refer to changes in relative reducing potential. Abbreviations: Z, the primary donor of PS II; P680, the PS II reaction center: Q, the primary acceptor of PS II; PQ, Plastoquinone; cyt. f., cytochrome f; PCy, Plastocyanin; P700, the PS I reaction center; X, the primary acceptor of PS I; Fd, ferredoxin; Fd-NADP red., ferredoxin-NADP reductase.

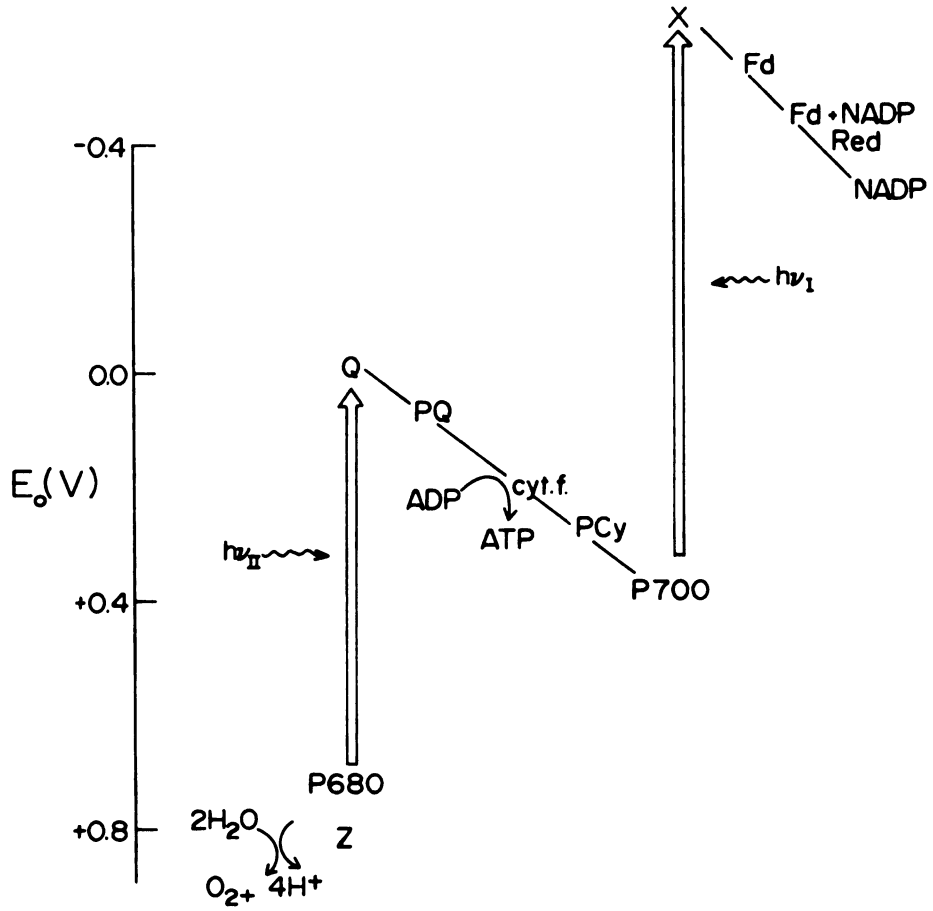
X
Fd
Fd + NADP
Red
NADP
-0.4
0.0
+0.4
+0.8
E_o(V)
$h\nu_I$
Q
PQ
ADP
cyt.f.
ATP
PCy
P700
$h\nu_{II}$
P680
$2H_2O$
Z
O_2+ 4H+

of a primary electron acceptor, Q, (E ~ 0.0 V) and the oxidation of P680 to $P680^+$. The species Q is thought to be a plastoquinone molecule. The subsequent reduction of $P680^+$ leads to the production of a strong oxidant, Z^+, (E ~ +0.8 V) which is as yet unidentified chemically, capable of oxidizing water to molecular oxygen.

Similarly, light energy absorbed by the antenna pigments of PS I is trapped at a reaction center which contains another photo-oxidizable form of chlorophyll, P700. Again, its name describes its absorption maximum near 700 nm. Charge separation at the PS I reaction center leads to the oxidation of P700 (E ~ +0.4 V) and the reduction of a primary electron acceptor, X, (E ~ -0.6 V). The reduced form of Q in PS II and the oxidized form of P700 in PS I are re-oxidized and re-reduced as a result of electron transfer along the electron transport chain connecting the two photosystems. The net result of the photoexcitation of these two photosystems is the transfer of electrons from water to the species X which then mediates the reduction of NADP. This links the oxidation of water to the formation of NADPH, a species used to fuel the enzyme cycles associated with the assimilation of CO_2 in the dark, exothermic reactions of photosynthesis.

An important property of the photosynthetic light reactions that is not evident from the Z scheme is its vectorial nature. The photosynthetic organelle of higher plant photosynthesis is the chloroplast. The pigments and enzymes required for the light dependent reactions are localized on the membranes of flattened sacks within the chloroplast called thylakoids. The thylakoid membrane, as part of a closed vesicle, separates two chemically different environments,

the outside or matrix side from the inside. The distribution of the photosynthetic components within the membrane is asymmetric, giving rise to a directionality in the electron flow. These asymmetric electron transport reactions result in both charge and proton gradients across the photosynthetic membrane which ultimately provide the free energy required for ATP synthesis (Mitchell, 1966; Neumann and Jagendorf, 1964). Figure 2 is a representation of the thylakoid membrane which incorporates membrane asymmetry in a schematic manner. The exact placement of the components is an area of very active current research, making the arrangement shown in Figure 2 tentative. Nonetheless, it is consistent with most of the experimental results reported to date. Those factors especially pertinent to the understanding of PS II are the presence of the plastoquinone pool and the location of P680 and Z toward the inside of the thylakoid. Plastoquinone serves as a secondary electron acceptor in the sequence of reactions following the photooxidation of P680. Each molecule of plastoquinone can accept two electrons as well as two protons from the chloroplast matrix. The lipid soluble reduced plastoquinone may then diffuse through the membrane, deliver two electrons to the next acceptor, currently though to be cytochrome f, along the electron transport chain joining the two photosystems and finally release two protons to the interior of the thylakoid. This results in the net influx of two protons for each molecule of plastoquinone reduced and subsequently re-oxidized. Another source contributing to the accumulation of protons within the thylakoid is the oxidation of water. For every mole of molecular oxygen produced, four moles of

Figure 2. A representation of the thylakoid membrane showing component asymmetry. Abbreviations: chl a, antenna pigments; Z, the primary donor of PS II; P680, the PS II reaction center; Q, the primary acceptor of PS II; PQ, the transmembrane, plastoquinone pool; cyt. f., cytochrome f; PCy, plastocyanin; P700, the PS I reaction center; X, the primary accepter of PS I; Fd,ferredoxin; Fd-NADP Red., ferredoxin-NADP reductase.

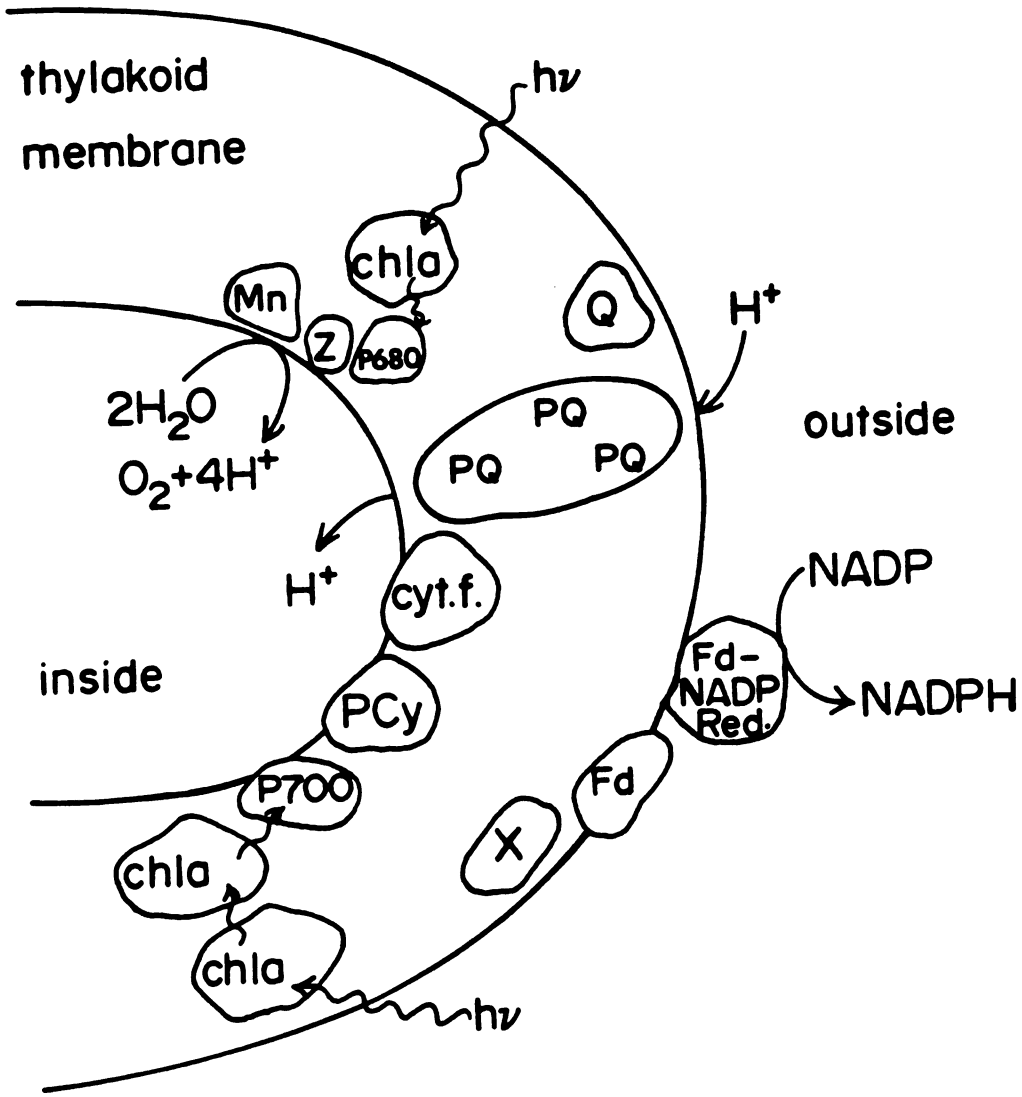
thylakoid
membrane
hν
chla
Mn
Z
P680
Q
H+
2H2O
O2+4H+
PQ
PQ
PQ
outside
H+
cyt.f.
NADP
inside
Fd-
NADP
Red.
NADPH
PCy
P700
Fd
X
chla
chla
hν

protons are released to the inside of the thylakoid. Through these two proton translocation sites, as well as others associated with PS I, a proton concentration gradient is established and maintained across the membrane.

Of the two light harvesting systems, the understanding of PS II has evolved more slowly than that of PS I. Indeed, as recently as 1966, the photoreaction of PS II was described as the "inner sanctum" of photosynthesis (Kok and Cheniae, 1966). Fortunately, since then advances have been made and although knowledge of the electron transport pathways and the photochemical reaction remains incomplete, the following model of the PS II reaction sequence has evolved:

$$1)\quad \text{chl}_a + h\nu \rightarrow \text{chl}_a^*$$

Light absorption by antenna chlorophyll.

$$2)\quad \text{chl}_a^* + \text{P680 Q} \rightarrow \text{chl}_a + \text{P680}^*\text{Q}$$

Transfer of excitation energy from the antenna chlorophyll to the reaction center.

$$3)\quad \text{P680}^*\text{Q} \rightarrow \text{P680}^+\text{Q}^-$$

Charge separation at the reaction center.

$$4)\quad \text{Z P680}^+\text{Q}^-\text{R} \rightarrow \text{Z}^+\text{P680 Q}^-\text{R}$$

Electron transfer from donor Z to P680.

$$5)\quad \text{Z}^+\text{P680 Q}^-\text{R} \rightarrow \text{Z}^+\text{P680 Q R}^-$$

Electron transfer to secondary acceptor R linked to plastoquinone pool.

$$6)\quad S_n + Z^+ \rightarrow S_{n+1} + Z$$

Charge accumulation, n=0, 1, 2, 3.

$$7)\quad 2H_2O + S_4 \rightarrow 4H^+ + O_2 + S_0$$

Oxygen evolution.

Reactions 1) and 2) occur in picoseconds, 3) in less than 20 nanoseconds, 4) in less than a microsecond and 5) with a half-time of about 600 microseconds. A brief description of reactions 6) and 7) follows.

Measurements by Joliot et al. (1969, 1971) and Kok et al. (1970) of oxygen evolution produced by short (duration less than 10 μs) saturating flashes show that the amount of oxygen produced by chloroplasts that have been in darkness for 15 min is different for each flash. Little or no oxygen is produced by the first two flashes and a maximum is observed after the third flash. A continued series of flashes gives a damped oscillation with a period of four when oxygen yield is plotted against flash number. These results have been interpreted by Kok et al. (1970) in the following scheme:

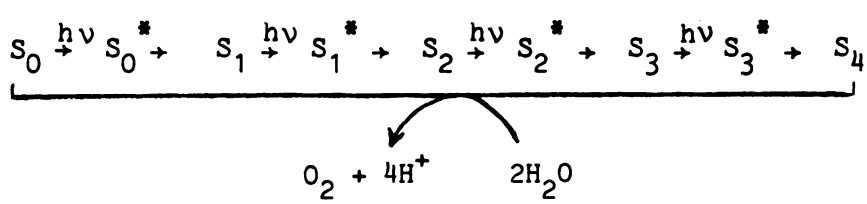

The steps $S_n \xrightarrow{h\nu} S_n^*$ represent phototransitions and the steps $S_n^* \rightarrow S_{n+1}$ are the subsequent dark electron transfer steps. The kinetics of these charge transfer reactions are slow compared to the 10 μs flash duration, hence the ability of a single flash to promote a

single electron transfer. Oxygen evolution occurs after storage of four oxidizing equivalents. The maximum yield of oxygen after the third flash indicates that most of the reaction centers are in the S_1 state after dark adaptation. It has been postulated that both the S_0 and S_1 states are stable in the dark and exist in a ratio of 1 to 3. The damping of the oscillatory pattern arises from "misses", a percentage of failures to produce charge separation at each reaction center (roughly 10% per flash). Little is known about the oxygen evolving step except that it has been shown that membrane bound manganese is involved (Cheniae and Martin, 1966; Blankenship and Sauer, 1974). Presumably, the charge accumulating reactions correspond to oxidation of the manganese species, although no firm experimental evidence exists to support this supposition.

The kinetic data and the model described above are based on data gathered by four techniques, oxygen evolution in flashing light and fluorescence, luminescence and absorption spectroscopy. Fluorescence emission with a quantum yield of about 0.03 is observed in functioning chloroplasts. Duysen and Sweers (1963) have demonstrated that the reduction and oxidation of Q, the primary electron acceptor of PS II, causes a corresponding increase or decrease in the fluorescence yield of the antenna chlorophyll. Oxidized Q is associated with low chlorophyll fluorescence, an observation which has led to the assignment of the term "quencher" to the species Q. An additional hypothesis, proposed by Butler et al. (1973) on the basis of experiments at 77 K, is that not only Q but also $P680^+$ quenches fluorescence. This postulate explains the low fluorescence yield observed

for both the P680 Q and $P680^+Q^-$ states. Although the range of validity of this working hypothesis has not been rigorously established, it is a useful tool in the study of $P680^+$ reduction kinetics. Immediately after a flash, when the system is in the $P680^+Q^-$ state, the fluorescence yield is low, due to the quenching of $P680^+$. The fluorescence yield will subsequently rise due to reaction 4) which leads to $Z^+P680\ Q^-R$, a state with no quenchers. The kinetics of the rise in fluorescence are interpreted as the rate of reduction of $P680^+$.

Another method of studying the kinetics of P680 is through luminescence or delayed light emission, which gives a typical quantum yield of 10^{-4} to 10^{-5}. Lavorel (1975) has hypothesized that the delayed light arises from the recombination reaction:

$$P680^+Q^- \rightarrow P680^*Q \rightarrow P680\ Q + h\nu$$

The species $P680^+$ is the lowest excited singlet state of P680. Dark regeneration of this state leads to the delayed emission of light. Luminescence intensity is then proportional to the concentration of $P680^+Q^-$. Since Q^- is re-oxidized much more slowly than $P680^+$ is reduced, the decay rate of the luminescence is proporational to the reduction rate of $P680^+$.

Another technique used in the study of P680 kinetics is absorption spectroscopy. Until recently, no absorption changes attributable to the reaction center of PS II could be observed under physiological conditions. At low temperatures or in the presence of detergents, the reduction of photooxidized P680 and the re-oxidation of Q^- can be slowed down. Floyd et al. (1971) observed a bleaching at 680 nm

upon illumination of chloroplasts with short laser pulses at 77 K. This absorbance change decays with a half-time of 4-5 ms upon darkening. Von Gorkom et al. (1974) observed the photooxidation of P680 in chloroplasts treated with the detergent deoxycholate and in the presence of ferricyanide, have found that the reduction of $P680^+$ is slowed to such an extent that an appreciable amount of $P680^+$ can actually be accumulated under conditions of continuous illumination.

Recent work done by Van Best and Mathis (1978) allows the study of the reduction kinetics of $P680^+$ at physiological temperatures. Their development of a flash absorption photometer with nanosecond time resolution has made this possible. They have found a fast (30 ns) decay time for $P680^+$, reflecting its reduction by the secondary electron donor. Of all of the techniques mentioned, this is the only one which measures a kinetic rate on the oxygen evolution side of P680. It is the intent of this study to investigate an additional means of collecting data directly from the electron transport system used to reduce $P680^+$.

The recent observation and characterization of an EPR detectable species (Babcock and Sauer, 1975; Blankenship et al., 1975) provides an excellent tool in studying these complex kinetics. The EPR active species appears to function as an intermediate in the electron transport process between $P680^+$ and the S_n states. In active, oxygen evolving chloroplasts, this signal is observed within 20 μs of an actinic flash. Its decay, under steady state illumination conditions of roughly one flash per second, has a half-time of about 600 μs. However, upon inhibition of oxygen evolution, brought about by TRIS

washing or exposure to heat, the decay rate falls dramatically to give a half-time of about 1 s. Introduction of artificial electron donors (phenylenediamine, hydroquinone, benzidine) to the inhibited chloroplast suspensions accelerates the decay process. The rapidly decaying signal from uninhibited chloroplasts has been named signal II_{vf} (very fast) while the signal associated with the inhibited chloroplasts has been named signal II_f (fast). It is the eventual intent of this research project to determine if both signals arise from one species, Z, the variation in decay kinetics reflecting the nature of the final electron donor. That is, if Z^+ is reduced by the water oxidizing enzyme complex (S_n states) and water, then signal II_{vf} if observed. If, however, water oxidation is inhibited, then Z^+ is reduced by endogenous electron donors and signal II_f is observed. It if can be shown that these two signals arise from a common species which exists as an intermediate in the electron transport chain between P680 and the S_n complex, an experimental observable will be available for the first time for the study of the complex reactions which lead to the photosynthetic evolution of oxygen.

In the initial experiments designed to probe this system, we have carried out a study of the effect of pH variation on the overall process of oxygen evolution. Parameters which complicate this process, particularly the membrane pH gradient, have been explored. Analogous experiments which use the EPR detectable species as a probe for electron transfer kinetics on the water side of PS II have been carried out.

I. The pH Dependence of Photosynthetic Oxygen Evolution

A. Introduction

The study of oxygen evolution as a function of pH is especially important since one effect of the light reactions of photosynthesis is the establishment and maintenance of a proton gradient across the thylakoid membrane. Variation of the pH of the suspension medium also offers a convenient and systematic way to perturb the system.

Membrane processes, however, complicate the system to some extent since protons are released to the interior of the thylakoid during the water oxidation reactions. Simultaneously, protons are carried through the membrane by the plastoquinone pool. The overall result is a pH gradient across the membrane. In normally functioning chloroplasts, phosphorylation reactions, ADP + P_i → ATP, are coupled to the efflux of protons from the thylakoid interior and dissipate the pH gradient (Mitchell, 1966). During chloroplast isolation, however, the soluble phosphorylating factors are removed. To prevent excessive acidification of the thylakoid interior, uncoupling agents have been used to replace the function of phosphorylation (Good, 1960; Hanstein, 1976). Because PS II is effectively isolated from PS I by this treatment, the addition of an exogenous electron acceptor is also necessary. In the experiments described below, we have investigated oxygen evolution as a function of pH and uncoupler mode of action.

B. Materials and Methods

1. Light Source and Optical Arrangement

The continous light source for this series of experiments is a General Electric 200 watt projection lamp. The intensity of the light reaching the sample is 5.8×10^5 erg cm^{-1} s^{-1} as determined

by a calibrated PIN 8 photocell. The light is passed through a heat absorbing filter (2 in x 2 in, Corning) and focused on the reaction chamber by a pair of planoconvex lenses. A set of neutral density filters (Balzer) allows controlled attenuation of the light incident on the reaction chamber.

2. Reaction Chamber and Oxygen Probe

The reaction chamber is a lucite cylinder of .75 cm radius and 6 cm height encased in a lucite cube (7.5 cm on a side) through which is flowed controlled temperature water from a model 2095 bath circulator (Forma Scientific). A lucite plug seals the reaction chamber after addition of the reactants. The tip of the oxygen probe lies flush with the side of the reaction chamber and perpendicular to the path of the light to prevent direct illumination of the electrodes. The probe, model YSI5331, Yellow Springs Instrument Company, consists of a platinum cathode and a silver anode which are bathed by a KCl solution held in place by a Teflon membrane bound to the probe tip. When a polarizing voltage is applied across the probe, the oxygen in the vicinity of the cathode is reduced according to the reaction:

$$O_2 + 2H_2O + 4e^- \rightarrow 4OH^-$$

The corresponding anode reaction is:

$$4Ag + 4Cl^- \rightarrow 4AgCl + 4e^-$$

Current flows in direct stoichiometric relation to the rate of oxygen reduction. As the oxygen is depleted in the region adjacent to the cathode, oxygen in solution diffuses through the Teflon membrane

at a rate proportional to its concentration. To insure a uniform oxygen concentration throughout the reaction chamber, constant stirring is provided by a synchronous motor operating a small magnetic stir bar in the sample chamber.

3. Detection and Recording Circuits

The circuit used to provide a bias to the electrode and to detect oxygen evolution is shown in Figure 3. The main component is a current to voltage transducing operational amplifier (Signetics-μA741). The output voltage is recorded as a function of time on a Sargent recorder model TR S-72190. A schematic representation of the oxygen evolution detection system is shown in Figure 4.

4. Spinach and Chloroplast Suspensions

The spinach used in these experiments is laboratory grown in a growth chamber (Environmental Growth Chambers). The plants are subjected to day and night cycles of 10 hours of light followed by 14 hours of darkness. The spinach is grown in an inert vermiculite base, the nutritional requirements being met by watering them with Modified Hoagland's Nutrient Medium (Hoagland and Brayer, 1936). The temperature in the growth chamber is maintained at 16°C. A simple and rapid process for chloroplast preparation is used (Babcock and Sauer, 1973). The chlorophyll concentration is determined by the method of Sun and Sauer (1971).

5. Experimental Protocol

In the dark, 3.5 ml of reaction solution is placed in the reaction chamber. This solution is 20 m$\underline{M}$ in NaCl, 5 m$\underline{M}$ in $MgCl_2$, 1 m$\underline{M}$ in $K_3Fe(CN)_6$, 1 m$\underline{M}$ in $K_4Fe(CN)_6$, 50 m$\underline{M}$ in buffer and 10 m$\underline{M}$ in

Figure 3. Oxygen evolution detection and recording circuit.

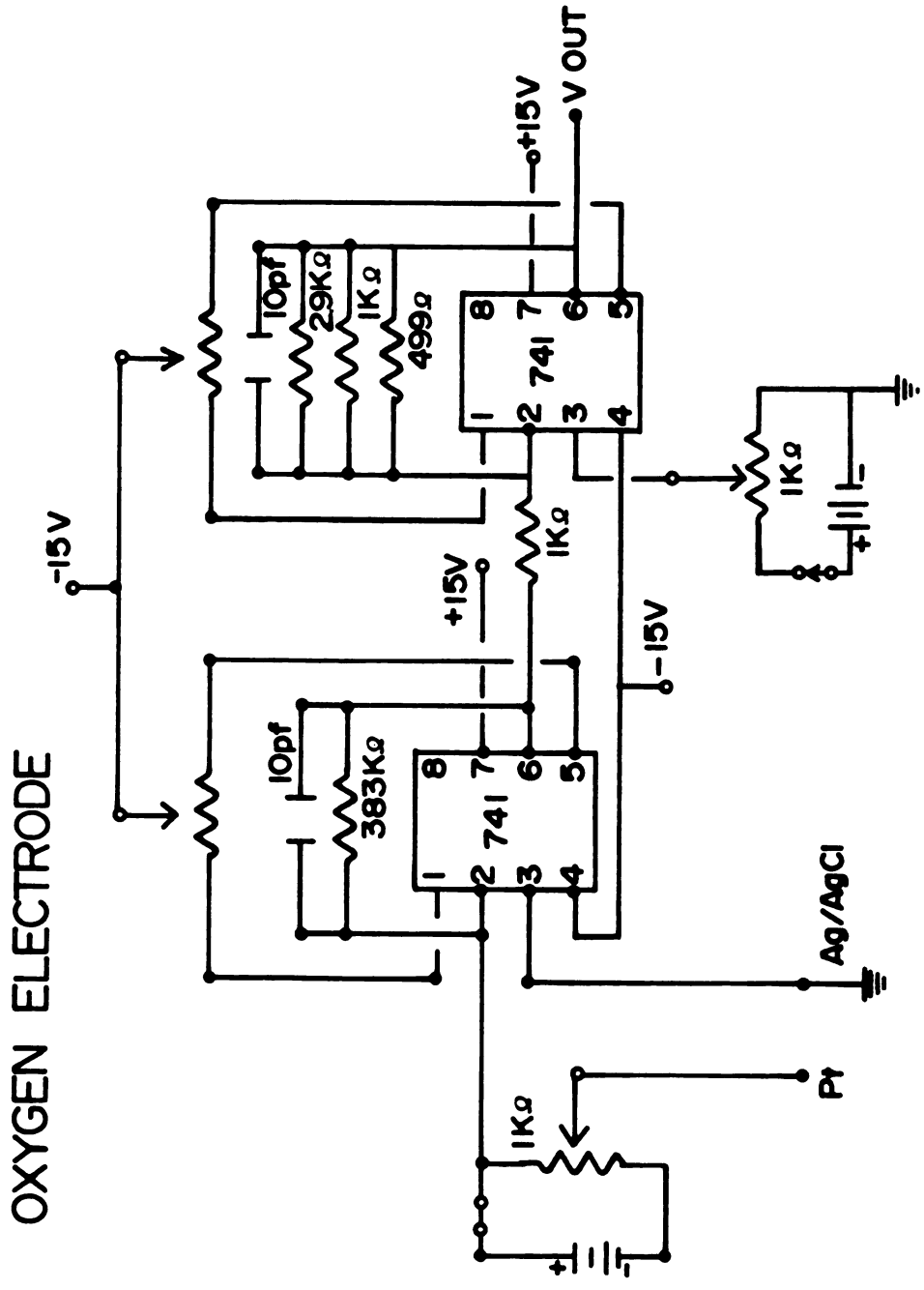
OXYGEN ELECTRODE
-15V
+15V
V OUT
10pf
29KΩ
1KΩ
499Ω
741
1KΩ
1KΩ
+15V
-15V
10pf
383KΩ
741
Ag/AgCl
1KΩ
Pt

Figure 4. Schematic representation of the oxygen evolution detection system.

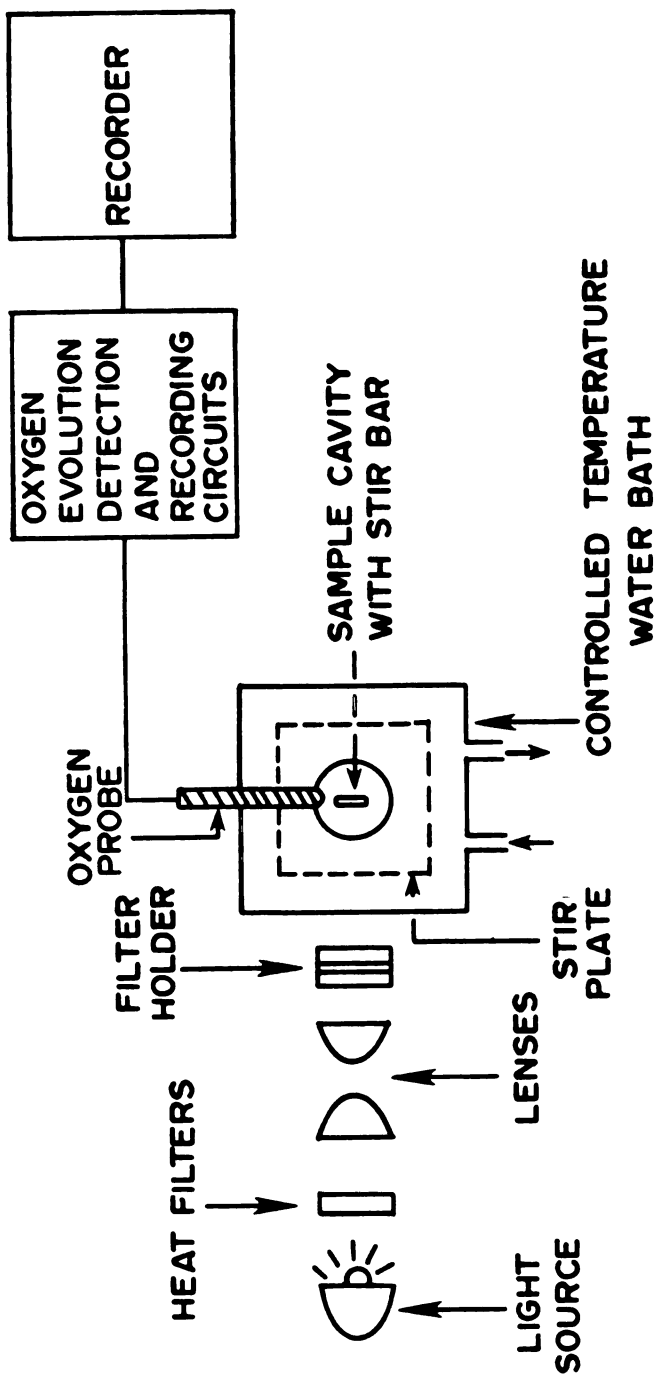
RECORDER
OXYGEN EVOLUTION DETECTION AND RECORDING CIRCUITS
SAMPLE CAVITY WITH STIR BAR
CONTROLLED TEMPERATURE WATER BATH
OXYGEN PROBE
FILTER HOLDER
STIR PLATE
HEAT FILTERS
LENSES
LIGHT SOURCE

uncoupling agents. The choice of buffer depends on the pH value to be maintained. For pH values of 5.5, 6.0 and 6.5, the buffer used is MES with a pKa of 6.1. For pH values of 7.0 and 7.5, the buffer used is HEPES with a pKa of 7.5. For pH values of 8.0 and 8.5, the buffer used is TRICINE with a pKa of 8.1. An aliquot of the chloroplast suspension is added to the reaction solution to give a final chlorophyll concentration of 10 μg per ml solution. This solution is kept in the reaction chamber in the dark for five minutes to allow the system to equilibrate and reach temperature stability. During the last minute a dark baseline is recorded. The sample is then illuminated and the oxygen evolution time course recorded for about 30 s. A strict adherence to this protocol gives values that are reproducible to within 4%.

C. Results

1. Polarogram

The value of the polarizing voltage to be applied so that maximum electrode sensitivity and stability are attained can be determined by measuring a polarogram. Ideally, the polarogram of voltage vs. current will have a diffusion controlled plateau region where variations in the applied voltage produce no variation in the current flow. Figure 5 shows the current vs. EMF relationship for air saturated buffer. The output signal is essentially invariant between -0.7 V and -1.0 V. A polarizing voltage of -0.8 V was selected. All polarographic voltages are reported relative to the Ag/AgCl electrode.

Figure 5. Polarogram of air saturated buffer.

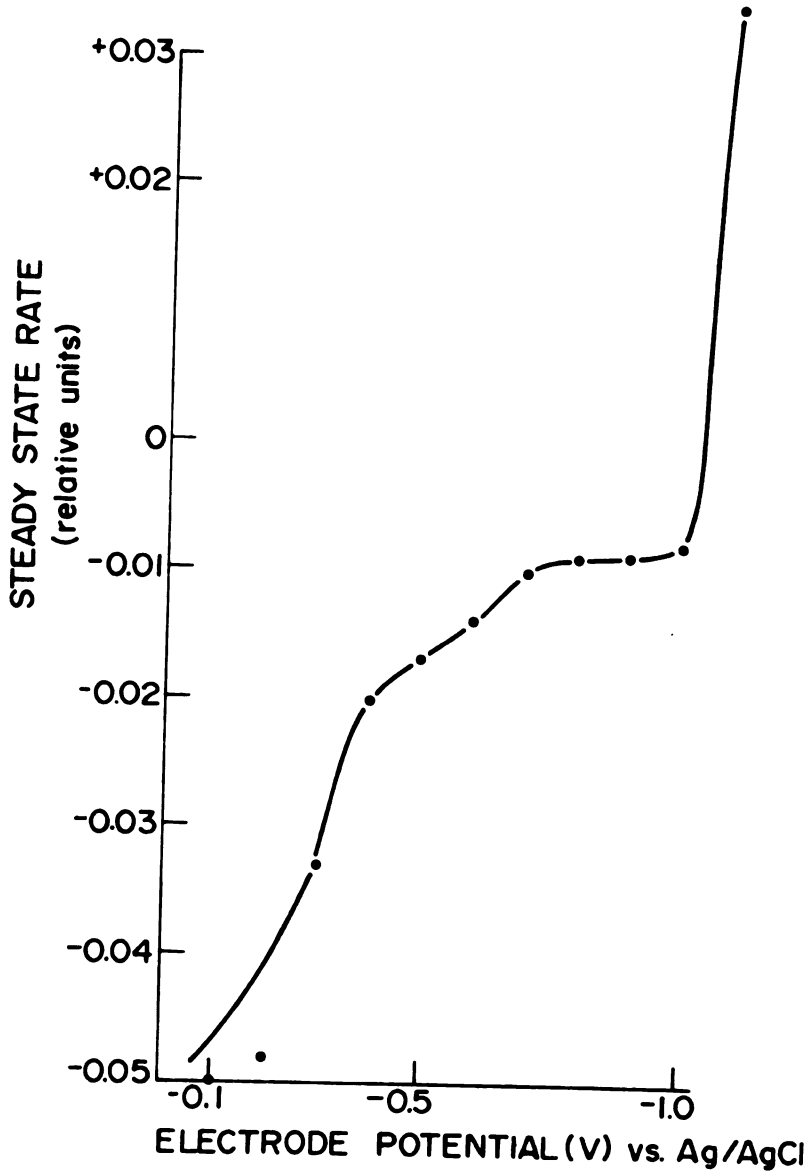
+0.03
+0.02
0
-0.01
-0.02
-0.03
-0.04
-0.05
STEADY STATE RATE
(relative units)
-0.1
-0.5
-1.0
ELECTRODE POTENTIAL (V) vs. Ag/AgCl

2. Calibration of the Electrode

In order to standardize the results of the oxygen evolution experiments, the electrode must be calibrated and the voltage readings converted to moles of oxygen evolved. This conversion can readily be made since the current produced by the electrode is a linear function of oxygen concentration. It is known that at 25°C, N_2 saturated water is 0.0 m$\underline{M}$ in O_2, O_2 saturated water is 1.143 m$\underline{M}$ in O_2, and air saturated water is 0.240 m$\underline{M}$ in O_2. The steady state voltage measured with each of these three solutions is plotted against the concentration of O_2 in each. The slope of this line is the conversion factor needed and has a value of 166.65 mV/m$\underline{M}$ O_2 for the electrode used in the experiments below (Figure 6).

3. Saturation Curve

To arrive at the proper light intensity and chlorophyll concentration, light intensity vs. oxygen evolution rate measurements were carried out. Conditions were varied until saturating light intensities were observed (Figure 7).

4. The pH Dependence of Oxygen Evolution

The results of the oxygen evolution experiments are shown in Figure 8, a plot of the observed rates of oxygen evolution vs. pH for three experimental systems; one using ammonia as the uncoupling agent, a second using methylamine and a third using gramicidin. These data are in good agreement with those of others (Holt and French, 1948; Renger et al., 1977). In all cases, the relative rate of oxygen evolution increases with increasing pH to a maximum rate at about pH = 7.0. At higher pH values, the rate falls off

Figure 6. Calibration curve for the oxygen electrode.

CALIBRATION OF THE ELECTRODE

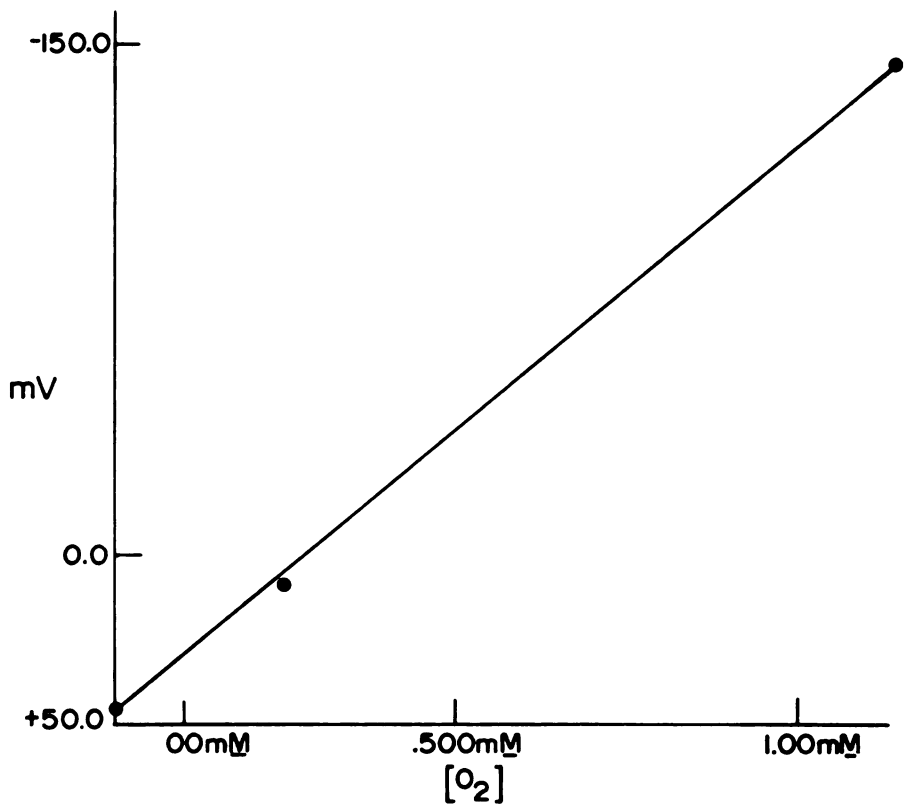

$$\text{SLOPE} = -166.65 \frac{\text{mV}}{\text{mmol } O_2 l^{-1}}$$

Figure 7. Saturation curve.

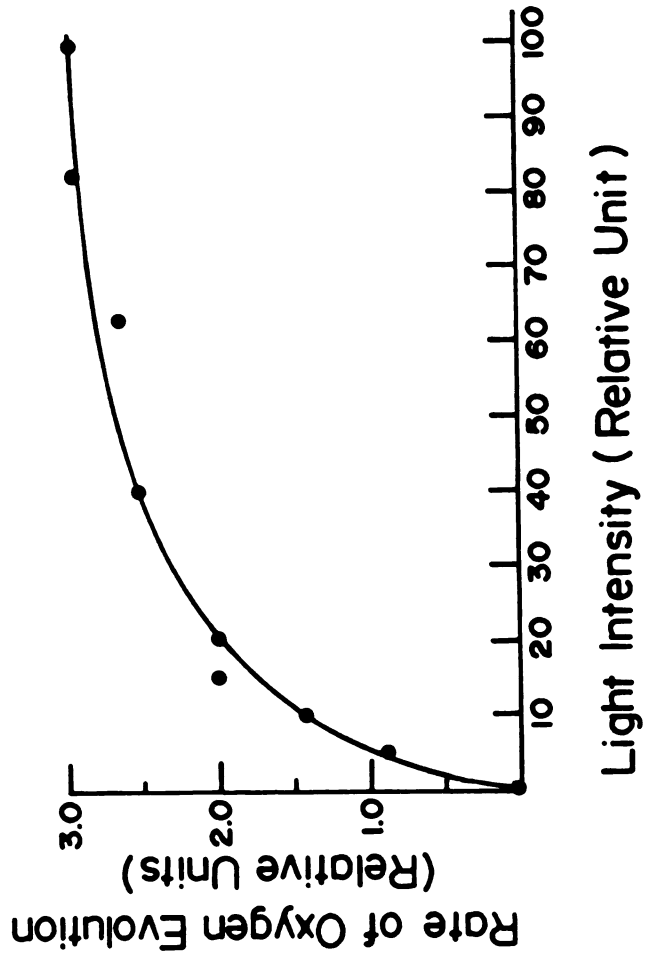
Rate of Oxygen Evolution
(Relative Units)
3.0
2.0
1.0
10
20
30
40
50
60
70
80
90
100
Light Intensity (Relative Unit)

Figure 8. Relative rates of oxygen evolution vs. pH for (●) a system uncoupled with 10^{-3} M NH_4Cl, (▲) a system uncoupled with 10^{-3} M CH_3NH_2, and (■) a system uncoupled with 10^{-6} M gramidicin.

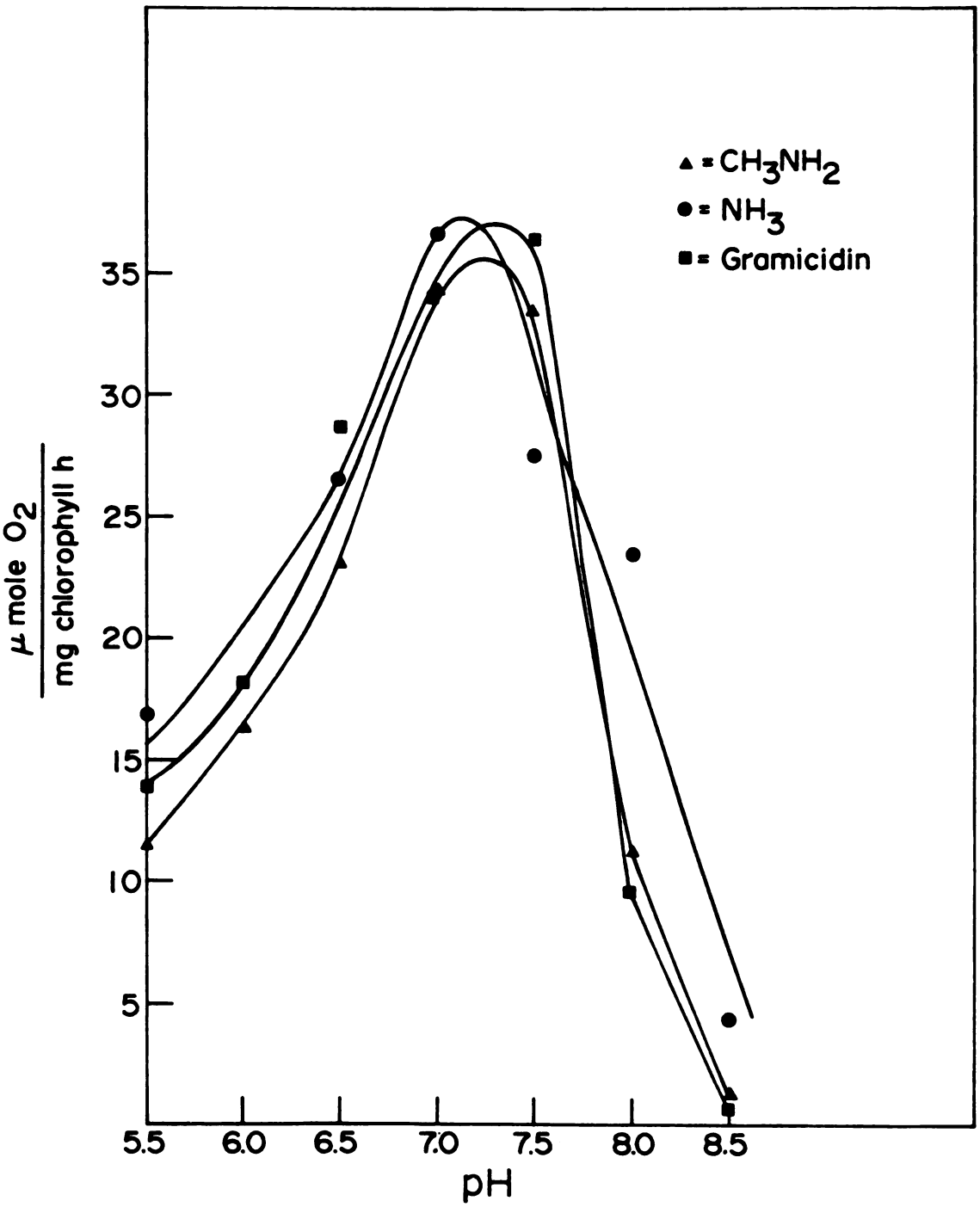
▲ = CH_3NH_2
● = NH_3
■ = Gramicidin
$\frac{\mu \text{ mole } O_2}{\text{mg chlorophyll h}}$
35
30
25
20
15
10
5
5.5
6.0
6.5
7.0
7.5
8.0
8.5
pH

dramatically. This loss of oxygen evolution can be explained as the inactivation at high pH values of the S_2 and S_3 states of PS II (Briantais et al., 1977).

D. Discussion

During photosynthetic oxygen evolution, a proton gradient is established across the thylakoid membrane by the translocation of protons from the matrix to the thylakoid interior and by the oxidation of water. It is possible to approximate the extent of this proton influx during the course of one experiment (30 s) from the measured rate of oxygen evolution. For the maximum rate observed, 1.02×10^{-8} moles of oxygen evolved in 30 s, about 1.64×10^{-7} moles of protons are released to the insides of the thylakoid membranes. An approximate volume for the total inner thylakoid space is 0.5 µl/ml suspension or about 1.75 µl under our experimental conditions (Siefermann-Harms, 1978). Using these values, we estimate that an internal pH of 1 would result from proton release. Before such a physiologically damaging pH could develop, the rate of oxygen evolution would fall. In order to allow oxygen evolution to continue at a measurable rate in isolated chloroplasts, uncoupling agents have been added to replace phosphorylation as the counter reaction to the proton influx.

One class of uncoupling agents, which has been found to be effective empirically, is amines. The neutral form of the amine is postulated to diffuse through the membrane to the interior where it may be protonated and act as an internal buffer (Crofts, 1967). A model is developed here to determine the internal buffering capacity

of various amines as functions of their pKa, their concentration and of the pH of the suspension medium. Our model depends on three assumptions:

1) Before illumination and the initiation of oxygen evolution, the amine concentration equilibrates across the membrane:

$$[RH]_i^* = [RH]_o^*$$

RH = neutral and protonated amine species.
* = before illumination
i = inside thylakoid.
o = outside thylakoid.

2) During oxygen evolution, the instantaneous concentration of the neutral amine on the inside and outside of the membrane is the same:

$$[R]_o = [R]_i$$

R = neutral amine.

3) For every mole of protons released to the interior of the thylakoid, one mole of neutral amine will be taken into the thylakoid from the suspension medium:

$$V[RH]_o = V[R]_o^* + V[RH^+]_o^* - H_p^+ = V[R]_o + V[RH^+]_o$$

$$v[RH]_i = v[R]_i^* + v[RH^+]_i^* + H_p^+ = v[R]_i + v[RH^+]_i$$

V = volume of the suspension medium.
v = volume of the inner thylakoid space.
RH^+ = protonated amine.

H_p^+ = the number of moles of protons that have been released to

the thylakoid interior as a result of photosynthetic reactions at the time the calculations are made.

Using these equations along with the pKa and concentration of the amine and the pH of the suspension medium, one may calculate the internal pH as a function of the external pH. The difference between these two values is known in the literature as ΔpH.

Figure 9 is a plot of calculated ΔpH vs. external pH for ammonium chloride (pKa = 9.249), methylamine (pKa = 10.569) and a hypothetical amine with a pKa of 7.0. If the external pH exceeds the pKa of the amine, the ΔpH deviates strongly from unity and the internal pH is no longer linearly related to the external pH. However, both ammonium chloride and methylamine maintain a ΔpH close to unity over the experimental pH range (5.5 - 8.5). These observations, based on the model developed here, explain the experimental observation that only amines with high pKa values are effective uncoupling agents (Schuldiner et al., 1971). It also explains why common buffers such as phosphate, HEPES, TRICINE and TRIS, with pKa values in the range 7.0 - 8.0, do not interfere with the phosphorylation process. Figure 10 is a plot of amine concentration vs. ΔpH. As the amine concentration increases, pH approaches zero and the internal pH asymptotically approaches the external pH. Qualitatively, these calculated data agree quite well with experimental values obtained in a study in which no theoretical model was proposed (Rottenberg and Grunwald, 1972). The ammonium ion concentration used in our experiments is 10^{-2} M. A more concentrated solution, which would lower the ΔpH, was not used as it has been reported that high ammonium ion concentrations inhibit oxygen evolution (Delrieu, 1976).

Figure 9. A plot of ΔpH vs. pH for amines with different pKa values.

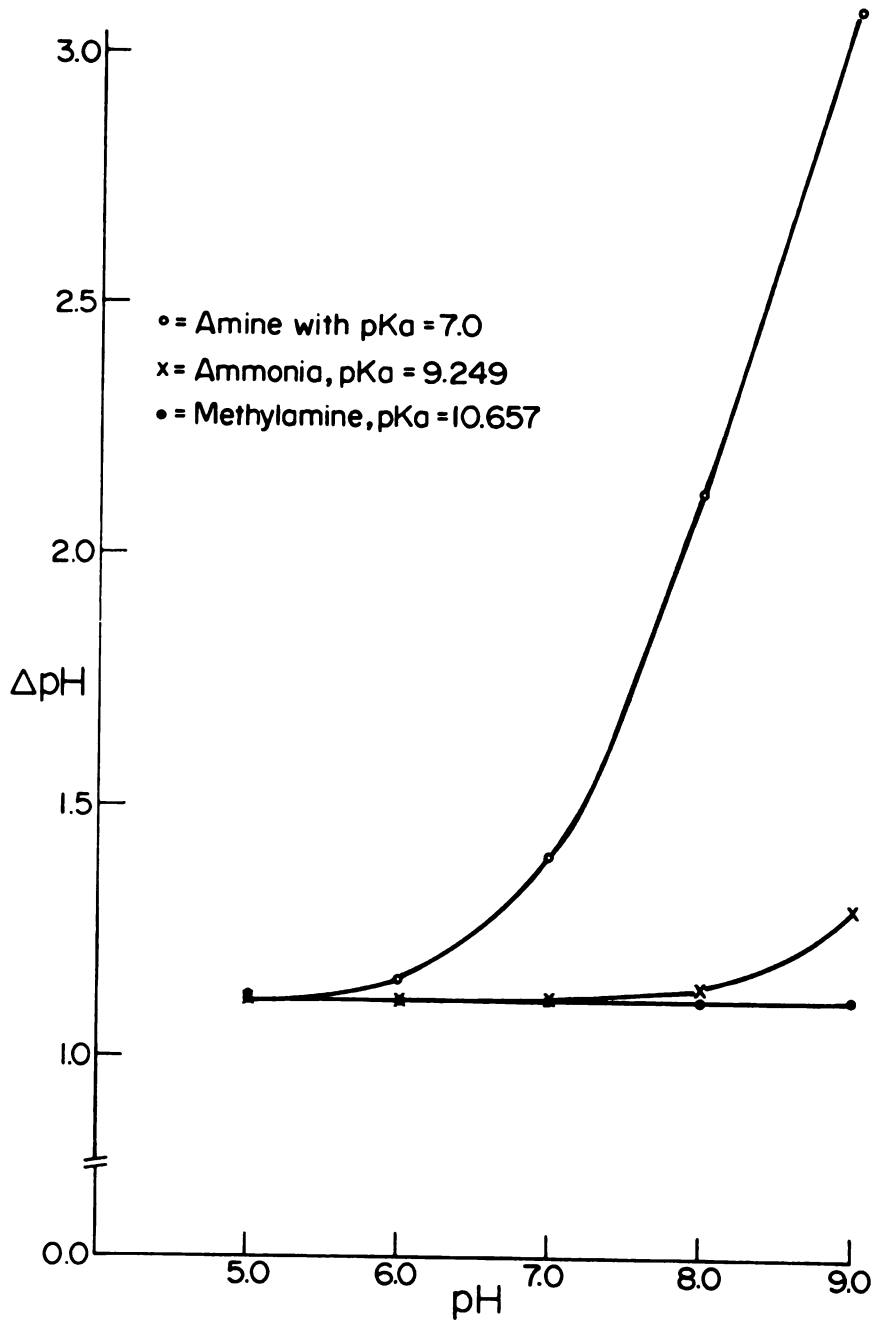
3.0
2.5
2.0
1.5
1.0
0.0
ΔpH
∘ = Amine with pKa = 7.0
x = Ammonia, pKa = 9.249
• = Methylamine, pKa = 10.657
5.0
6.0
7.0
8.0
9.0
pH

Figure 10. A plot of amine (CH_3NH_2) concentration vs. calculated ΔpH.

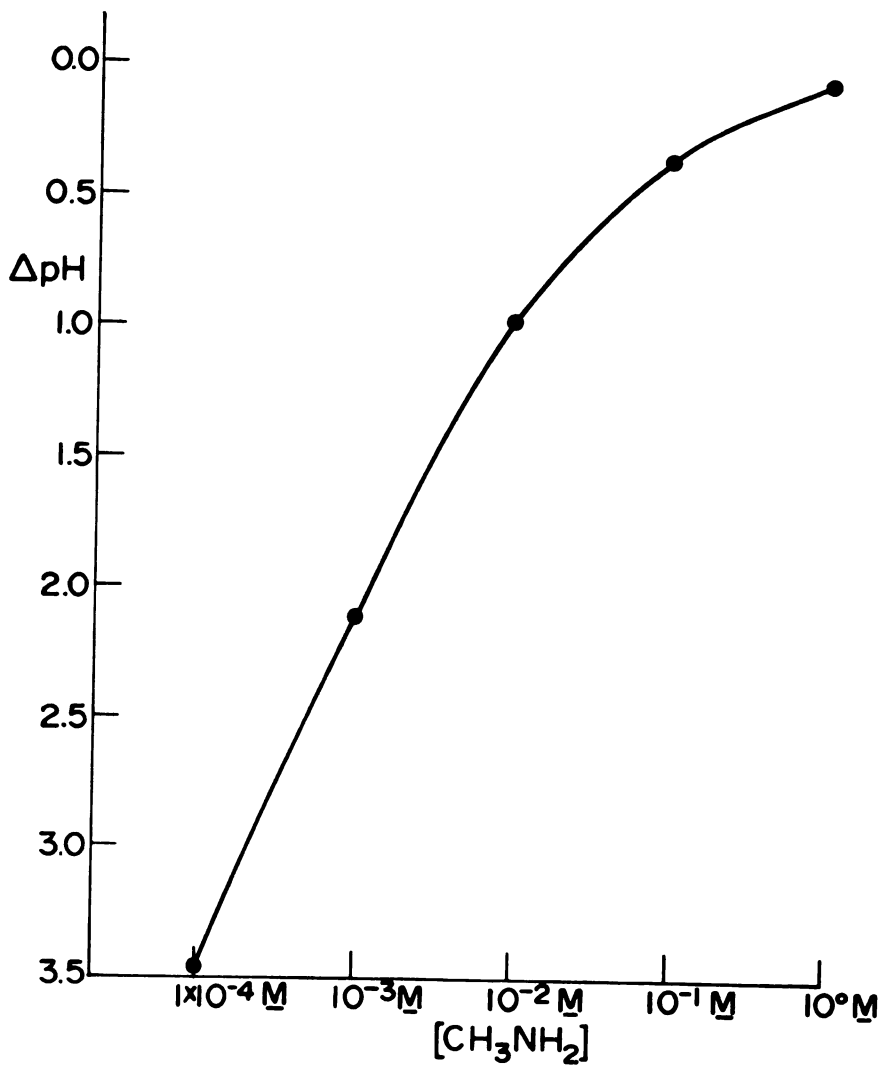
0.0
0.5
ΔpH
1.0
1.5
2.0
2.5
3.0
3.5
1x10-4 M
10-3M
10-2 M
10-1 M
10° M
[CH3NH2]

The experimental results (Figure 8) show a definite relationship between observed rates of oxygen evolution and the pH of the suspension medium. Through our model we have determined that the efficiency of the uncoupling amine is relatively independent of the pH of the suspension medium when the pKa of the amine is sufficiently high (Figure 9). If this were not the case, however, the observed pH dependence of oxygen evolution might reflect an artifactual pH dependence of this system, perhaps in the rate of amine incorporation into the thylakoid. At low pH values, the concentration of the neutral amine in the suspension medium would be correspondingly low which could lead to a lower rate of transport across the membrane, a less efficient internal buffering capacity and eventually to a lower rate of oxygen evolution.

To test this possibility, the experiments have been repeated using an uncoupling agent that works by an entirely different mechanism. The agent chosen is the antibiotic, gramicidin, which has been shown to uncouple phosphorylation by increasing the permeability of the membrane toward cations (Junge and Witt, 1968; Shavit et al., 1968). The photosynthetically induced proton gradient is dissipated by the outward diffusion of protons through the hydrophilic pores that result upon the incorporation of gramicidin into the membrane. Oxygen evolution experiments using gramicidin as the uncoupling agent show the same pH dependence as those using amines (Figure 8). This leads to the conclusion that the incorporation of the amine is not the rate determining, pH dependent step in amine uncoupled oxygen evolution.

The other component which could lead to an artifactual pH dependence is the exogenous electron acceptor, ferricyanide. Experiments by Itoh (1978) have shown that ferricyanide is photoreduced by a component of the electron transport chain linking the two photosystems. Itoh found that low pH values lead to higher rates of ferricyanide reduction. Based on this observation, he suggested that the ferricyanide reduction site is buried within the membrane and that negative charges at the membrane surface impede the diffusion of ferricyanide to the site. At low pH values, the surface charges are shielded, allowing easier access to the site. This pattern of decreasing rates of ferricyanide reduction with increasing pH is opposite to the trend observed in the oxygen evolution experiments where the reaction rate increases with increasing pH. Thus, ferricyanide reduction does not appear to be the pH dependent, rate limiting step of oxygen evolution in this system.

In these experiments, we have measured the pH dependence of oxygen evolution and obtained data in agreement with those of others (Holt and French, 1948; Renger et al., 1977). We have developed and tested a model to explain the uncoupler mode of action and to define more clearly the complicating role of the membrane. Using the model and experimental results, we have shown that the observed pH dependence is a true property of oxygen evolution and not merely an artifact of the system studied. It is, however, a macroscopic property. The following experiments are an attempt to further define its origin.

II. The pH Dependence of Signal II_f

A. Introduction

As described in more detail in the Introduction, this signal arises from a component on the water oxidizing side of P680. Its position in the electron transport sequence is shown in the scheme:

$$P680 \text{ —— } Z \text{ —— } S_n \qquad \overset{2H_2O}{\underset{O_2 + 4H^+}{\circlearrowright}}$$

where Z represents an unknown number of electron transport intermediates, one of which gives rise to an EPR signal. After photooxidation of P680, the Z species reduce $P680^+$. During this sequence, one intermediate becomes EPR detectable upon oxidation; its subsequent reduction can be observed as the decay of the EPR signal. In oxygen evolving chloroplasts, the case illustrated above, the final reducing agent is water. Under these conditions, the EPR signal observed is called signal II_{vf}. It has a rise time of less than 20 μs and a decay half-time of about 600 μs.

If, however, oxygen evolution is inhibited, the reaction sequence changes:

$$P680 \text{ —— } Z \overset{\text{inhibition}}{\dashv\vdash} S_n \qquad \begin{matrix} 2H_2O \\ O_2 + 4H^+ \end{matrix}$$

endogenous or exogenous

electron donors

The physiological electron transport pathway can be blocked by inhibitory techniques, among them TRIS washing, heating, aging or the addition of denaturants. These treatments release membrane bound manganese and result in the loss of oxygen evolution. Under these

conditions, the ultimate $P680^+$ reducing agent is no longer water, but endogenous or exogenous electron donors. Upon inhibition of oxygen evolution, the decay kinetics of the EPR signal are slowed considerably, the decay half-time changing to about 1 s. The EPR signal exhibiting these decay kinetics is called signal II_f. Addition of exogenous electron donors decreases the decay half-time.

B. Materials and Methods

1. Kinetic EPR Instrumentation

a. EPR Spectrometer, Signal Averager and Timing Circuits

All experiments are performed with a Varian model E-4 spectrometer using a transverse magnetic 110 mode cavity (Varian E238). The sample cell is a Scanlon flow EPR flat cell (S-814).

Because of the relatively low concentration of the paramagnetic species obtainable in the chloroplast suspensions, the time course for the transient rise and decay of the EPR detectable species must be enhanced through time averaging. Data are collected and stored with a Nicolet model 1074 signal averager. A plug in model SD-72/2A analog to digital converter and model SW-71A time base are used in the 1074 main frame.

A TTL logic-based timing circuit has been designed and built by the Michigan State University Chemistry Department electronics shop which allows us to trigger up to six different instruments at intervals continuously variable from 1 μs to 100 μs.

b. Laser

The laser head, containing the main discharge capacitor, flash lamp, pump and dye cell, is a model DL-1100 from Phase-R Corporation,

New Durham, New Hampshire. It is rated at 250 mJ output light energy with rhodamine 6G (λ_{max} = 590 nm) with a pulse duration of 450 ns. The 25 KV power supply has been built by the electronics shop. The triggering system, based on a schematic supplied by Phase-R, was further developed in our laboratory.

The first experiments using the laser light source revealed a large electrical transient, generated by the triggering of the laser, which obscured the EPR signal. The following shielding scheme evolved to separate the laser and EPR systems. The laser is in a Faraday cage with r.f. shielding (Instrument Specialities Co., Inc., Little Falls, New Jersey) at all of the joints. The two systems are grounded separately and are interfaced via opto-isolators whose circuit diagrams are shown in Figure 11. These measured have eliminated the electrical transient.

The dye used is a solution of cresyl-violate perchlorate and rhodamine 6G in methanol which emits at 660 nm, a wavelength close to the absorption maximum of the PS II reaction center (680 nm). The concentration and cresyl-violet to rhodamine ratio of the lasing solution have been determined experimentally to give optimum light intensity at moderate (16 KV) voltages.

c. Light Monitor and Filters

The light intensity may be monitored during the course of the experiment. The monitor is a glass plate between white surfaces with openings to allow most of the light to pass through. Part of the light is reflected by the plate glass surface and is then detected and integrated by four photodiodes (Hewlett-Packard) connected in

Figure 11. Circuit diagram for diode opto-isolator.

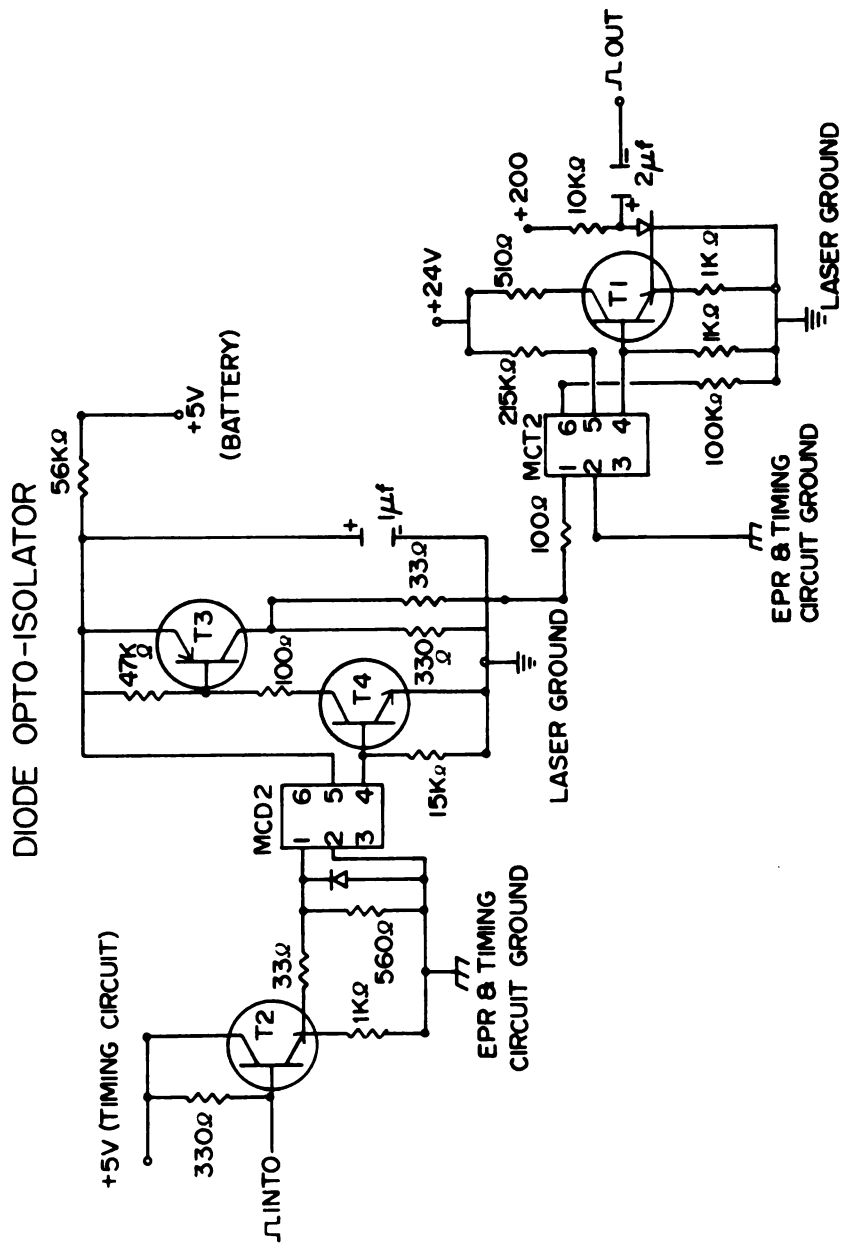
DIODE OPTO-ISOLATOR
56KΩ
+5V
(BATTERY)
1μf
33Ω
47KΩ
T3
100Ω
T4
330Ω
15KΩ
MCD2
LASER GROUND
100Ω
MCT2
215KΩ
+24V
510Ω
+200
10KΩ
2μf
OUT
T1
1KΩ
1KΩ
100KΩ
LASER GROUND
EPR & TIMING
CIRCUIT GROUND
EPR & TIMING
CIRCUIT GROUND
+5V (TIMING CIRCUIT)
330Ω
INTO
T2
33Ω
1KΩ
560Ω

parallel with a 820 pf capacitor (Van Best, 1977). The voltage across the capacitor can be read from an oscilloscope (B&K Precision model 1471B). This circuit is mounted on a filter holder also accomodating neutral density filters.

A block diagram showing the main components of the kinetic EPR instrumentation is shown in Figure 12. Because of limited time resolution in the present system, only the pH dependence of signal II_f decay kinetics will be studied. Modification of the lock-in amplifier (Princeton Applied Research model 126) shown in Figure 12 is now in progress which will decrease the time constant from about 800 μs to 50 μs. This should allow us to perform analogous experiments to study the pH dependence of signal II_{vf} decay kinetics.

2. Spinach and Chloroplast Suspensions

Market spinach is used in this series of experiments. Chloroplasts are prepared as described in Section I with the following modifications. After centrifugation, the chloroplasts are resuspended in 0.8 M (pH = 8.0) TRIS buffer and left exposed to light for twenty minutes. This procedure is referred to as TRIS washing and results in the release of manganese bound to the thylakoid membrane with the concomitant loss of oxygen evolution. The chloroplasts are centrifuged, washed in the reaction mixture which is 0.4 M in sucrose, 10 mM in NaCl, and 50 mM in buffer (MES for pH = 5.5, 6.0 and 6.5, HEPES for pH = 7.0 and 7.5 and TRICINE for pH = 8.0 and 8.5) and finally resuspended in a minimal volume of this mixture. The chloroplasts are maintained at $0^{o}C$ during this procedure.

Figure 12. Block diagram of kinetic EPR instrumentation.

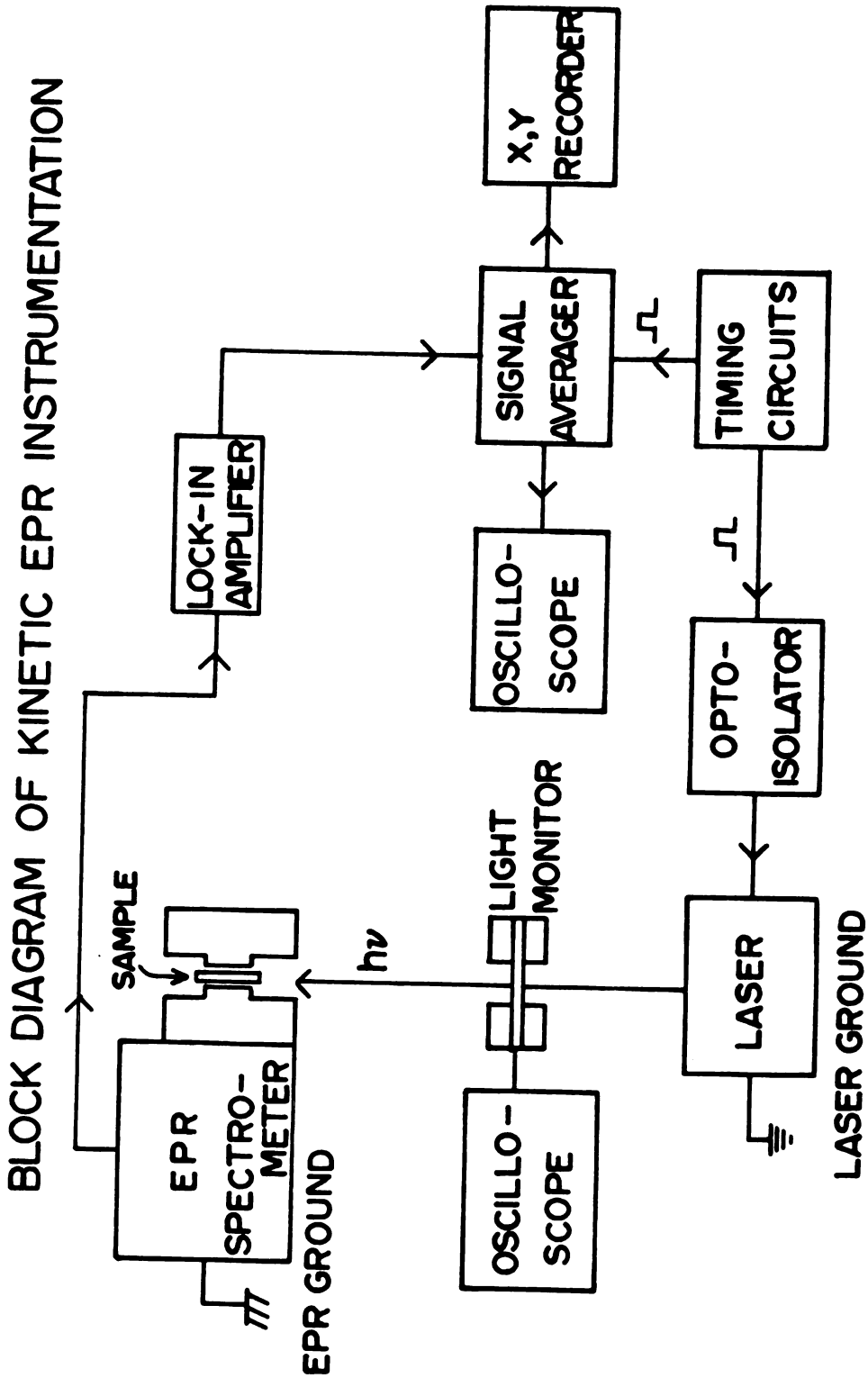
BLOCK DIAGRAM OF KINETIC EPR INSTRUMENTATION
EPR SPECTRO-METER
EPR GROUND
SAMPLE
hν
LIGHT MONITOR
LOCK-IN AMPLIFIER
OSCILLO-SCOPE
OSCILLO-SCOPE
SIGNAL AVERAGER
X,Y RECORDER
TIMING CIRCUITS
OPTO-ISOLATOR
LASER
LASER GROUND

3. Experimental Protocol

The chloroplasts are kept at $0^{o}C$. Before any experiments are run, stock suspensions for each pH value are made, each 10^{-4} M in EDTA which complexes Mn^{2+}, 5×10^{-4} M in NADP and with a ferredoxin concentration of 20 μg/ml of suspension. The NADP and ferredoxin constitute an electron acceptor system. Immediately prior to each experiment, exogenous donors (ascorbate, hydroquinone) are added to the stock suspension. The EPR sample cell is then filled, centered and the experiment begun. Six seconds are allowed between laser flashes to allow the chloroplasts to relax to the dark equilibrium state. The number of scans averaged is chosen according to the instrument time constant which is, in turn, determined by the rate of decay of the radical. These parameters are noted in the figure legends.

C. Results

1. Signal I and Signal II

At room temperature, two EPR detectable species are generated upon illumination of intact, oxygen evolving chloroplasts. The first, signal I, has rapid rise and decay kinetics and has been established as arising from $P700^{+}$, the photooxidized reaction center of PS I (Beinert and Kok, 1964; Kohl, 1972). The second, called signal II, is less well characterized. It has a line width of about 20 G and a decay time in the order of hours (Heise and Treharné, 1964). Chloroplast suspensions enriched in PS II activity show an increase in the magnitude of signal II (Kohl, 1972). Signal II has, therefore, been associated with PS II (Weaver, 1968). Inhibition of oxygen evolution by TRIS washing activates a component of signal II not

normally observed in chloroplasts. This component has been named signal II_f as it exhibits fast decay kinetics relative to signal II. Signal II_f exists in a 1:1 ratio with the slower decaying signal II species (Babcock and Sauer, 1975). Figure 13 shows EPR spectra of TRIS washed spinach chloroplasts during (a) and after (b) illumination. Upon darkening, signal I (I) decays rapidly. The behavior of the signal II species is noted on the figure.

2. Signal II_f

Figure 14 is a collection of kinetic traces of signal II_f decay under different experimental conditions. Figure 14-A is the decay transient observed from chloroplasts at pH = 7.5 in the absence of exogenous electron donors. Under these conditions, the decay kinetics are bi-phasic as demonstrated by Figure 15, a plot of the natural log of the signal II_f free radical concentration vs. time for the trace shown in Figure 14-A. In the absence of exogenous electron donors, the number, identity and concentration of the species that reduce the signal II_f radical are unknown, making interpretation of the data difficult. It is, however, likely that one of the endogenous donors is ascorbate. To define more clearly the conditions controlling signal II_f reduction kinetics, known concentrations of ascorbate have been added to the suspension medium.

Figures 14-B and C show the results of the addition of ascorbate as an exogenous electron donor at pH values of 6.5 and 7.5. The decay kinetics are much faster and exhibit a qualitative change as well. Figure 16 is a plot of the natural log of the signal II_f free radical concentration vs. time for the kinetic trace shown in Figure 14-B. The kinetics now show exponential decay characteristics.

Figure 13. EPR spectra of TRIS washed (pH = 6.5) chloroplasts during (a) and after (b) illumination. Field set = 3365 G, scan range = 100 G, modulation amplitude = 5 G, power= 20 mW.

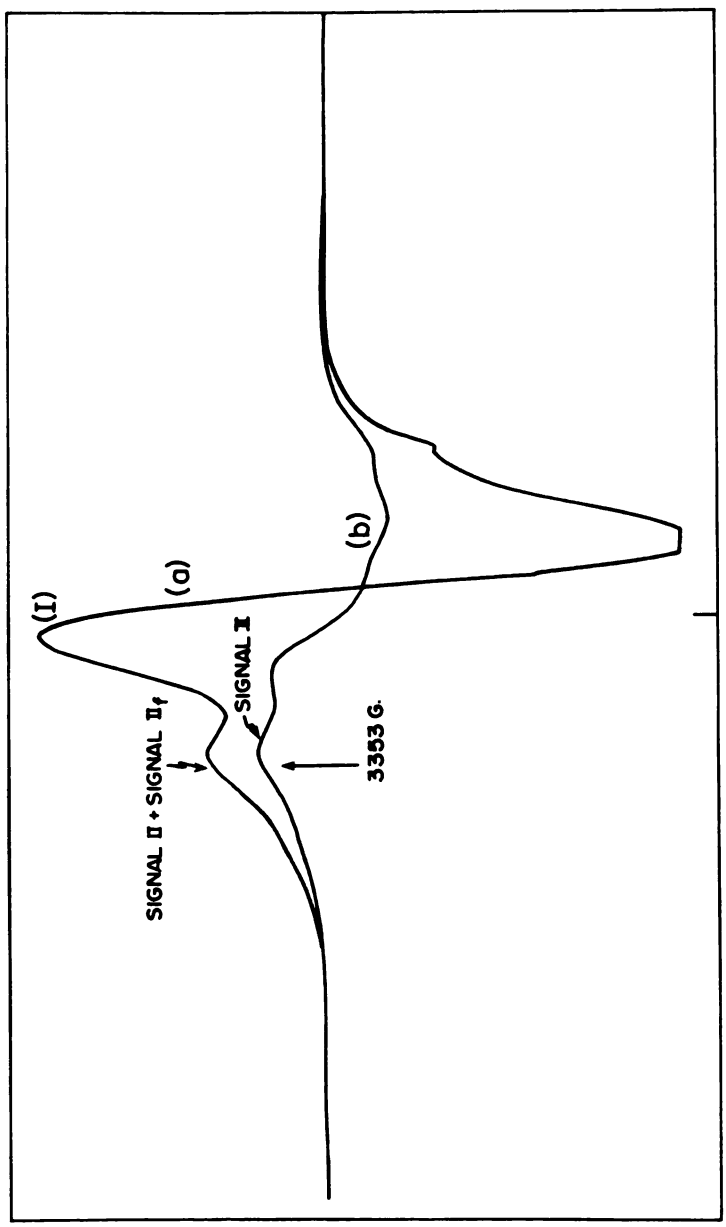
(I)
(a)
(b)
SIGNAL II + SIGNAL II'
SIGNAL I
3353 G.

Figure 14. The effect of exogenous electron donors on EPR signal II_f decay kinetics. All experiments were performed on TRIS washed chloroplasts to which 5 x 120^{-4} M NADP, 10^{-4} M EDTA and 20 µg ferredoxin/ml suspension had been added. The field setting for all experiments at 3353 G, the modulation amplitude is 5 G and the power is 20 mW. The scans were run at 6 s intervals.

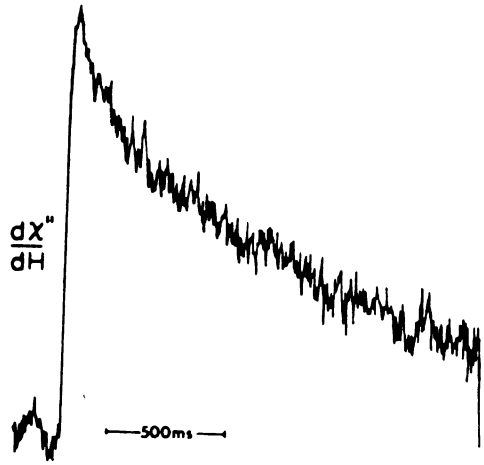

A. No further additions. pH = 7.5 (time constant = 10 ms, 64 scans averaged)

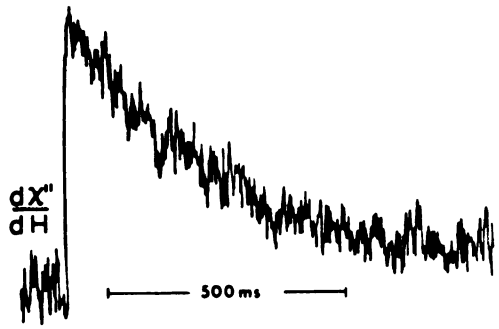

B. With 2×10^{-3} M ascorbate. pH = 6.5 (time constant = 3 ms, 120 scans averaged)

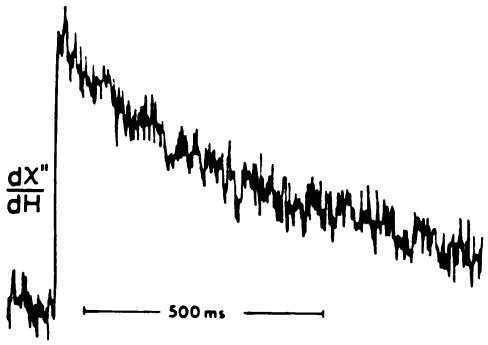

C. With 2×10^{-3} M ascorbate. pH = 7.5 (time constant = 3 ms, 120 scans averaged)

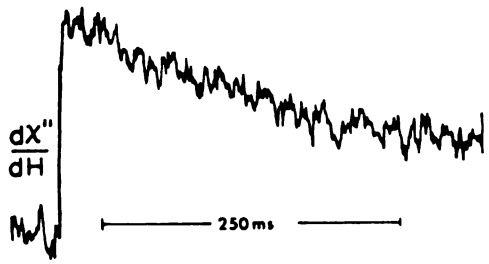

D. With 10^{-5} M hydroquinone and 2×10^{-3} M ascorbate. pH = 7.5 (time constant = 3 ms, 200 scans averaged)

Figure 15. A semi-log plot for the natural log of signal II_f concentration vs. time at pH = 7.5 in the absence of exogenous electron donors. The plot demonstrates the bi-phasic decay kinetics under these conditions.

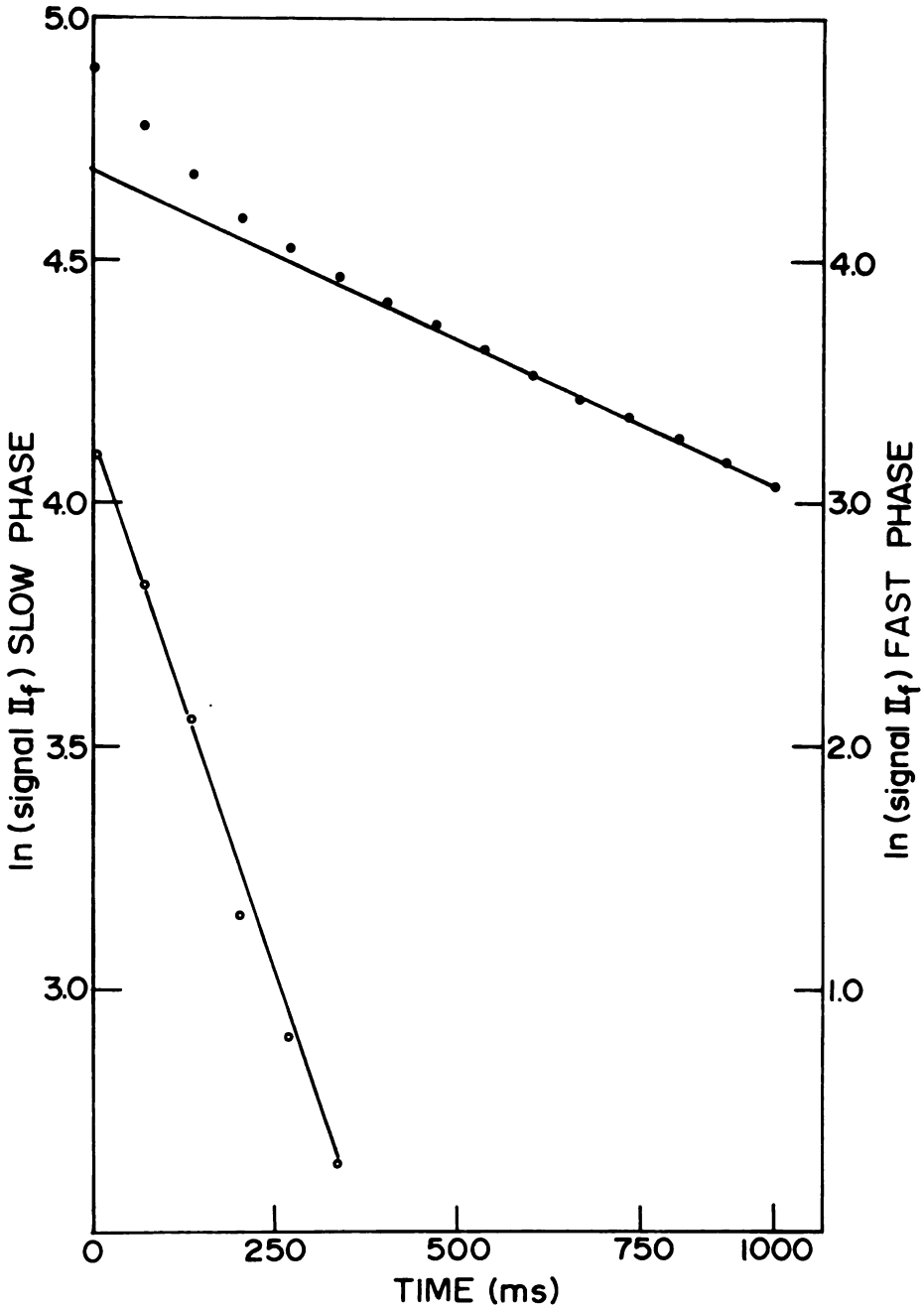
5.0
4.5
4.0
3.5
3.0
4.0
3.0
2.0
1.0
0
250
500
750
1000
TIME (ms)
ln (signal II_f) SLOW PHASE
ln (signal II_f) FAST PHASE

Figure 16. A semi-log plot of the natural log of signal II_f concentration vs. time at pH = 6.5 with an added ascorbate concentration of 2×10^{-3} M. The plot demonstrates the first order decay kinetics followed under these conditions.

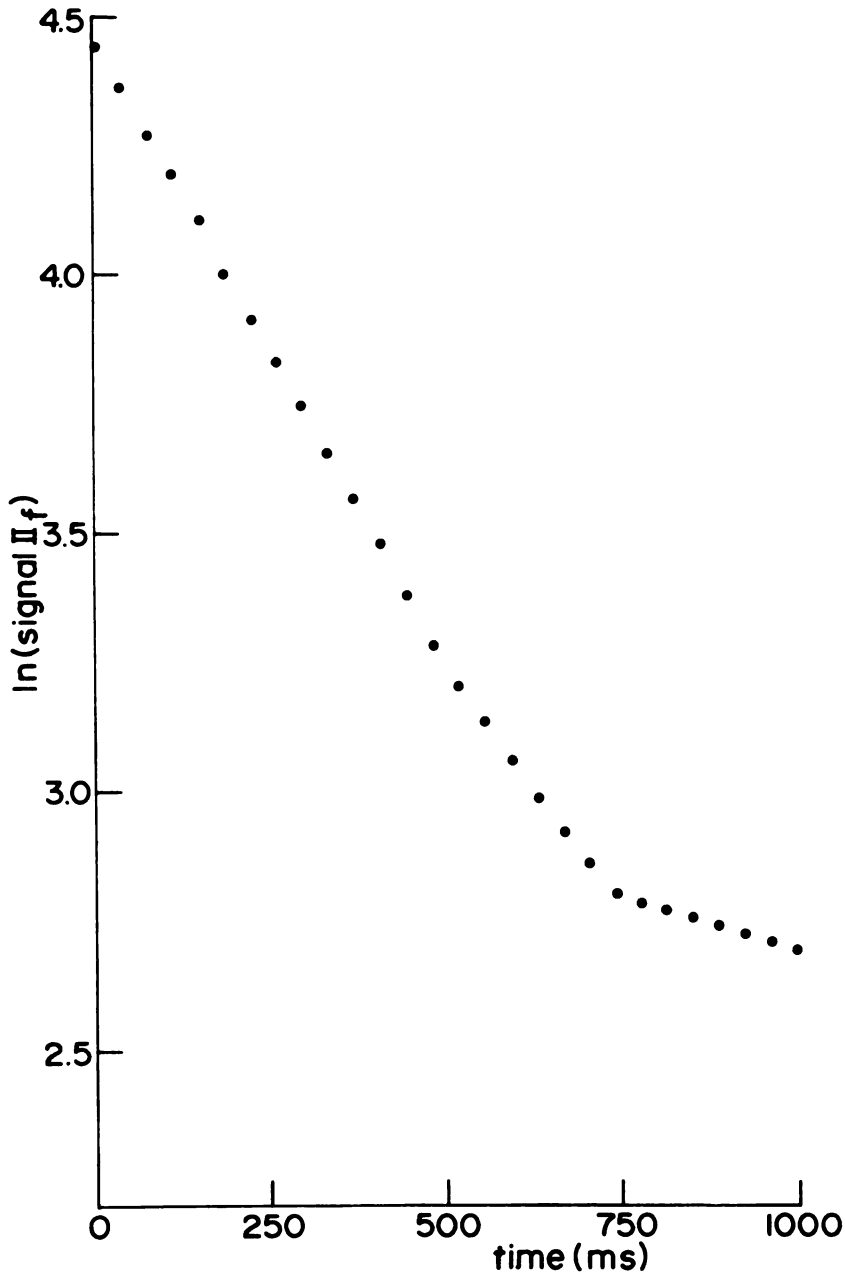
4.5
4.0
3.5
3.0
2.5
ln(signal Π_f)
0
250
500
750
1000
time (ms)

Similar plots at the other experimental pH values also reveal that the decay of signal II_f in the presence of added ascorbate follows first order kinetics. These observations suggest that at these ascorbate concentrations, signal II_f decay follows pseudo-first order kinetics and that the observed rate constant, k_{obs}, can be separated into the product of a second order rate constant and an essentially invariant concentration of ascorbate.

$$\frac{d[Z^+]}{dt} = k\,[Z^{\cdot+}]\;\;[HAsc]$$

$$k_{obs} = k\;\;[HAsc]$$

To investigate the implication of pseudo-first order kinetics, additional experiments were performed to relate the observed rate of decay of signal II_f to the concentration of added ascorbate. These results, at both pH = 6.5 and 7.5, are shown in Figure 17. The linear dependence at both pH values of the observed rate substantiates the proposed, pseudo-first order kinetic scheme.

A third set of experiments was performed using hydroquinone as the exogenous electron donor. Hydroquinone, with a pKa = 10.35, was chosen because it exists almost exclusively in its fully protonated state in the pH range used. This is in contrast to ascorbate (pKa = 4.10) which exists largely as an anion above pH 5.5. Figure 14-D is the trace obtained at pH = 7.5 with an added hydroquinone concentration of 10^{-5} M. At this low concentration, it was necessary to also add ascorbate (2×10^{-3} M) needed to reduce the hydroquinone after it is oxidized by the signal II_f radical. A further increase

Figure 17. A plot of the observed decay rate of signal II_f (k_{obs}) vs. concentration of ascorbate at two different pH values.

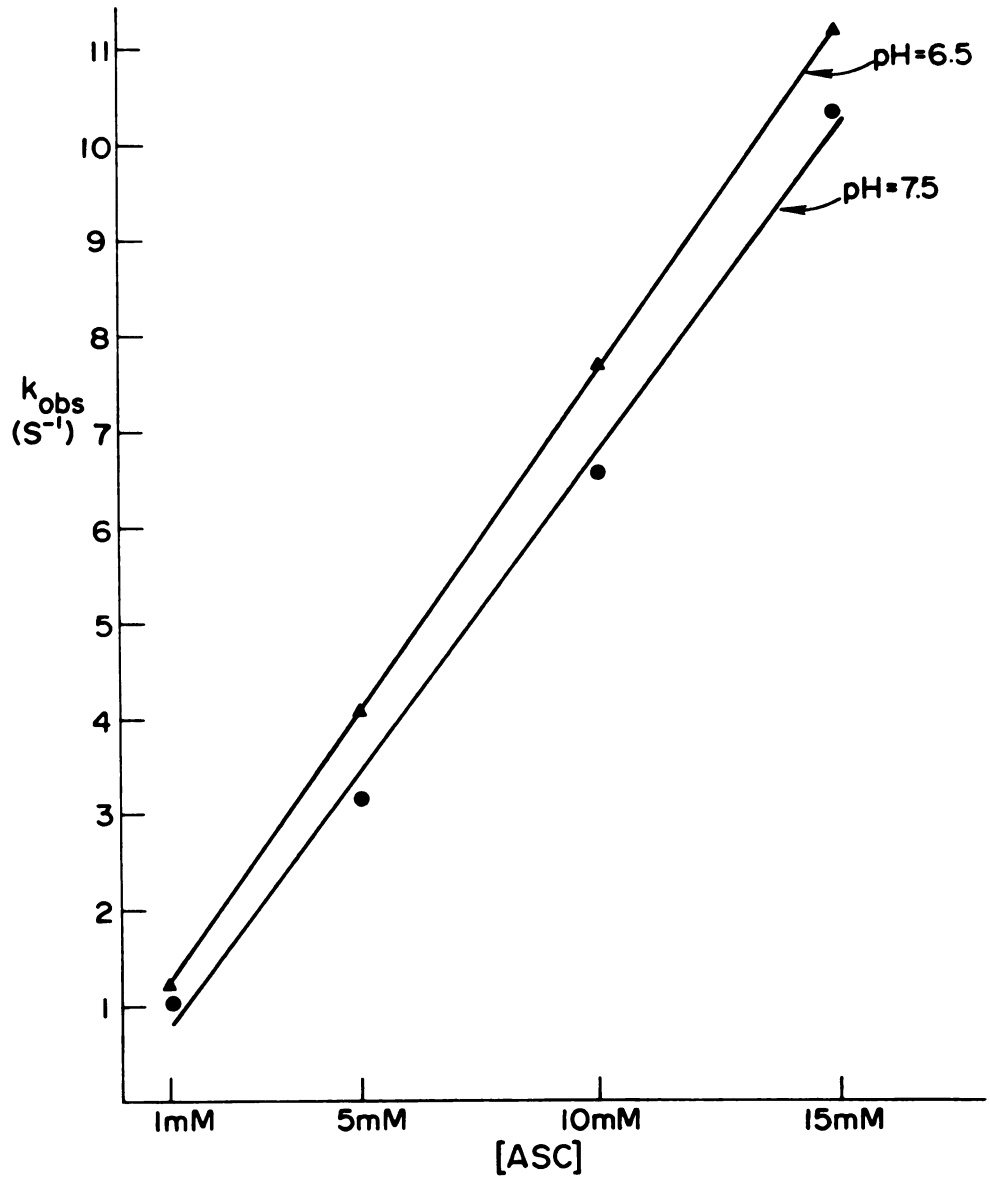
11
10
9
8
k_{obs} (S^{-1}) 7
6
5
4
3
2
1
pH=6.5
pH=7.5
1mM
5mM
10mM
15mM
[ASC]

in the rate of signal II_f decay is evident upon addition of hydroquinone. A semilog plot shows that the decay kinetics are first order.

Figure 18 summarizes the data obtained at all pH values in the presence of exogenous electron donors. It is a plot of the decay half-time vs. pH. An overall pattern of pH dependence in the decay kinetics of signal II_f emerges, the reduction of the paramagnetic intermediate being faster at low pH values.

D. Discussion

1. Endogenous Electron Donors

The results of the analysis of the kinetic traces obtained in the absence of exogenous donors are summarized in Table 1. In each case the decay of signal II_f can be analyzed as the sum of two, distinct decay processes, one fast and another relatively slow. By plotting the natural log of the signal II_f radical concentration vs. time, and by back extrapolating from the end of the time course, k_s, the slow rate constant can be determined from the slope and an amplitude, A_s, that proportion of the total signal following the k_s decay rate, can be approximated from the intercept at time zero. After subtracting the contribution made by this process from the overall observed rate, k_f, the rate constant for the fast process can be determined. These values are tabulated. Several conclusions can be reached from these data. The k_s, or slow decay rate constants, do not vary as strongly with pH as do the values of k_f, which tend to become appreciably faster at higher pH values. A second observation is that, as the pH is increased, a larger fraction of the total signal

Figure 18. A plot of signal II_f decay half-times vs. pH for three experimental systems; ( ) with 2 x 10^{-3} M ascorbate, (o) with 10^{-5} M hydroquinone and 2 x 10^{-3} M ascorbate and ( ) with 5 x 10^{-5} M hydroquinone and 2 x 10^{-3} M ascorbate.

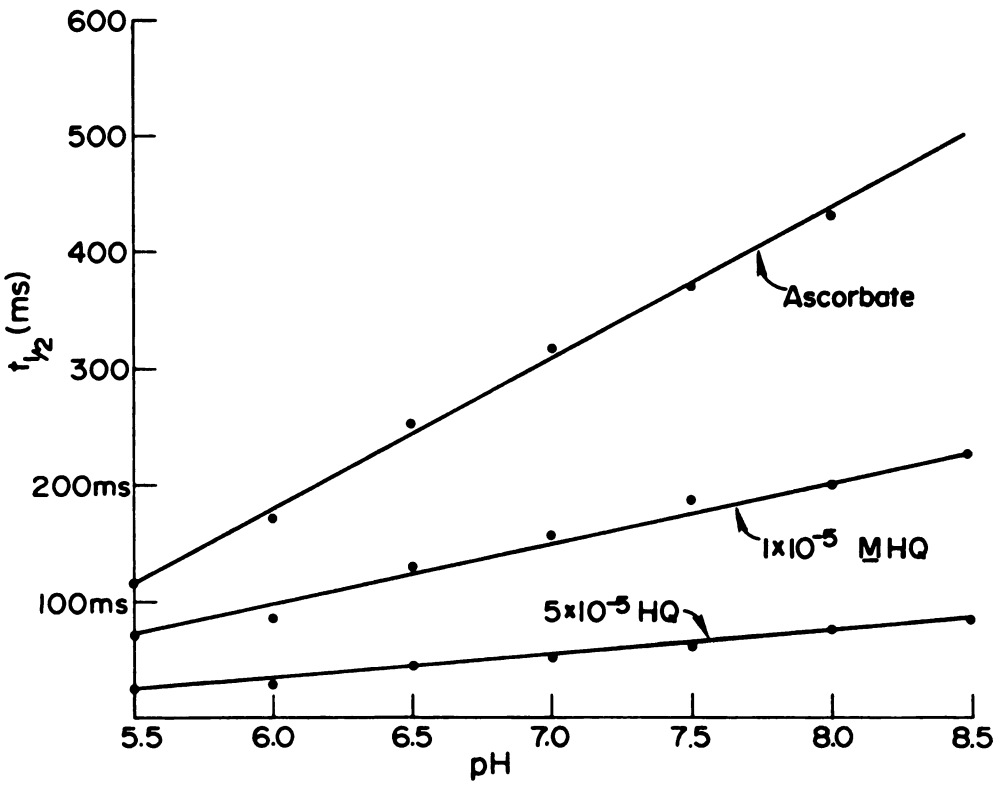
600
500
400
300
200ms
100ms
$t_{1/2}$ (ms)
Ascorbate
1×10^{-5} M HQ
5×10^{-5} HQ
5.5
6.0
6.5
7.0
7.5
8.0
8.5
pH

Table 1. A breakdown of the bi-phasic decay of signal II_f in the absence of exogenous donors; k_s = slow decay rate, k_f = fast decay rate, A_s = percentage of total signal following slow kinetics, A_f = percentage of the total signal following fast kinetics.

pH	k_s s^{-1}	A_s %	k_f s^{-1}	A_f %
5.5	.885	70.4	6.15	29.6
6.0	.948	65.2	4.73	34.6
6.5	.801	74.5	5.85	25.5
7.0	.814	82.9	5.13	17.1
7.5	.707	80.1	7.96	19.9
8.0	.744	86.5	9.48	13.5
8.5	.727	84.2	--	15.8

decays with the slower rate constant. Because the nature and concentration of the endogenous electron donors giving rise to these kinetics are unknown and experimentally uncontrollable, a more detailed analysis of these data has not been carried out.

2. Exogenous Electron Donors

The data presented in Figure 16 demonstrate that the decay of signal II_f, which reflects the reduction of a free radical, $Z^{+}\cdot$, proceeds by pseudo-first order kinetics in the presence of ascorbate. The rate constant calculated for this process is a function of pH (Figure 18). The following kinetic scheme can be used to rationalize these observations:

$$Z^{+}\cdot + HAsc \xrightarrow{k} Z + HAsc^{+}\cdot$$

where $Z^{+}\cdot$ is the free radical species giving rise to signal II_f and HAsc represents neutral ascorbate. The decay of signal II_f is given by:

$$\frac{-d[Z^{+}\cdot]}{dt} = k\ [Z^{+}\cdot]\ [HAsc]$$

The concentration of neutral ascorbate is related to the pH by:

$$H^{+} + Asc^{-} \underset{}{\overset{Ka}{\rightleftharpoons}} HAsc$$

If this were an accurate description of the kinetics, the observed rates, k_{obs}, would be proportional to the concentration of neutral ascorbate. Figure 19 is a plot of these two functions. At low pH values the agreement is good but the correlation falls off with increasing pH. This observation suggests a second model to explain the reduction kinetics of $Z^{+}\cdot$ as a function of pH:

Figure 19. A plot to the concentration of neutral ascorbate (solution 2 x 10^{-3} M in ascorbic acid) vs. pH (•) and a plot of k_{obs} vs. pH (o).

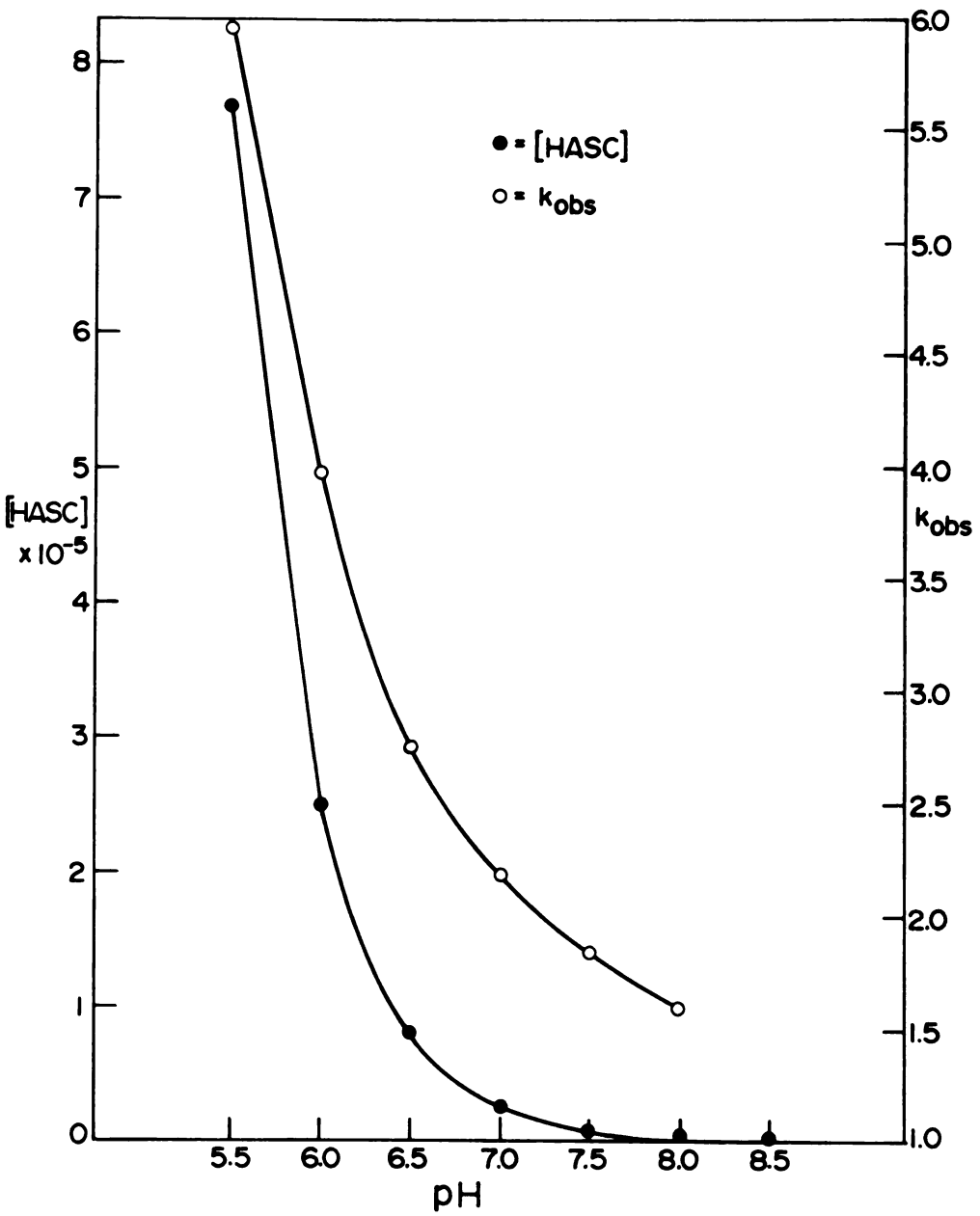
● = [HASC]
○ = k_{obs}
[HASC] x 10^{-5}
k_{obs}
pH
0
1
2
3
4
5
6
7
8
1.0
1.5
2.0
2.5
3.0
3.5
4.0
4.5
5.0
5.5
6.0
5.5
6.0
6.5
7.0
7.5
8.0
8.5

$$Z^{+}\cdot + HAsc \xrightarrow{k_1} Z + HAsc^{+}\cdot$$

$$Z^{+}\cdot + Asc^{-} \xrightarrow{k_2} Z + Asc\cdot$$

$$H^{+} + Asc^{-} \underset{}{\overset{Ka}{\rightleftharpoons}} HAsc$$

In this scheme, both neutral ascorbate and its anion reduce $Z^{+}\cdot$ and the decay of signal II_f is now given by:

$$\frac{-d[Z^{+}\cdot]}{dt} = k_1 [HAsc] [Z^{+}\cdot] + k_2 [Asc^{-}] [Z^{+}\cdot]$$

By introducing the ascorbate equilibrium this becomes:

$$\frac{-d[Z^{+}\cdot]}{dt} = k_1 \left[\frac{[H^{+}] [Asc^{-}]}{Ka} [Z^{+}\cdot]\right] + k_2 [Asc^{-}] [Z^{+}\cdot]$$

which reduces to:

$$\frac{-d[Z^{+}\cdot]}{dt} = [Z^{+}\cdot] [Asc^{-}] \left[\frac{k_1 [H^{+}]}{Ka} + k_2\right]$$

At low pH values, the H^{+} concentration is high and the k_1 kinetics will dominate. At high pH values, the H^{+} concentration is low and the k_2 kinetics will dominate. From experiments in which k_{obs} is obtained as a function of ascorbate concentration (Figure 17), the values of k_1 and k_2 can be calculated. The slopes of these plots can be used to calculate $d(k_{obs})/d[Asc^{-}]$ which is equal to $k_1 [H^{+}]/Ka + k_2$. Solving this set of equations leads to $k_1 = 1.4 \times 10^{4}$ $\underline{M}^{-1}$ s^{-1} and $k_2 = 6.6 \times 10^{2}$ $\underline{M}^{-1}$ s^{-1}.

These values of k_1 and k_2 have been used to calculate the overall decay rate of signal II_f as a function of pH and these calculated rates, k_{calc}, subsequently compared to the observed rates, k_{obs}. Figure 20 is a plot of k_{calc}/k_{obs} vs. pH for two sets of experimental data obtained with different preparations of chloroplasts. The relationship is linear in both cases but demonstrates a variable pH dependence. The validity of this kinetic scheme is supported by these results; the non-zero slope, however, is an indication that some subtle pH dependence has not been taken into account. Two such dependencies emerge as possibilities.

The first involves the concept of the transmembrane pH gradient or ΔpH as developed in Section I-D. In the calculation of the k_{calc} values, the H^+ concentration used in the rate expression is taken from the pH of the buffering medium. Based on the model developed in Section I-D, however, the pH inside of the thylakoid membrane will not be the same as that outside unless there is complete uncoupling of phosphorylation. Yamashita and Butler (1969) have shown that upon addition of electron donors, TRIS washed chloroplasts continue to undergo phosphorylation, an indication that a pH gradient develops during exogenous donor oxidation even after the inhibition of oxygen evolution. Using the rate expression, it is possible to calculate the internal H^+ concentration necessary to give the observed decay rates and from these concentrations and the pH values of the buffering medium, to further calculate a series of ΔpH values. These are plotted as a function of external pH in Figure 21. The ΔpH values obtained by this method are entirely reasonable and their increase

Figure 20. A plot of k_{calc}/k_{obs} for two different chloroplast suspensions.

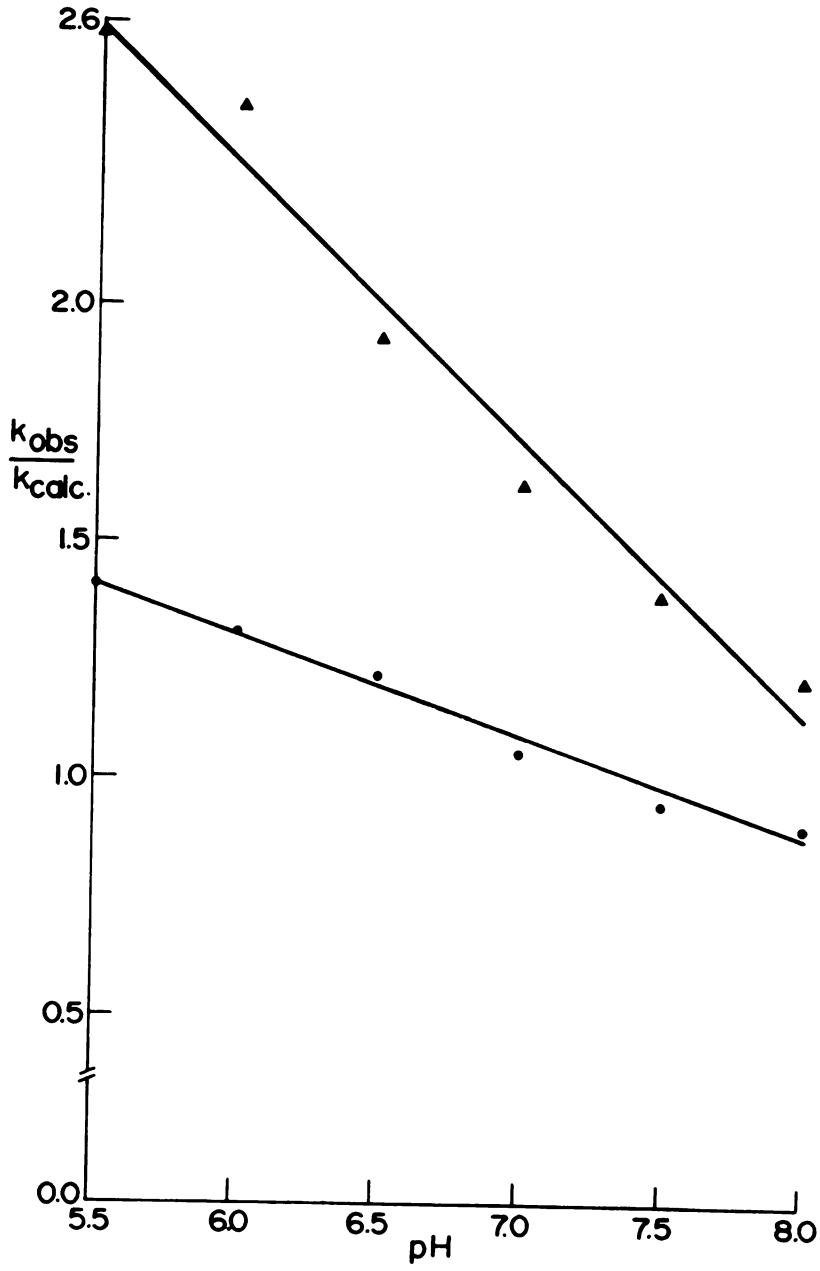
2.6
2.0
1.5
1.0
0.5
0.0
$\frac{k_{obs}}{k_{calc.}}$
5.5
6.0
6.5
7.0
7.5
8.0
pH

Figure 21. A plot of ΔpH vs. external pH calculated from the observed decay kinetics of signal II_f with 2×10^{-3} M ascorbic acid as an exogenous electron donor.

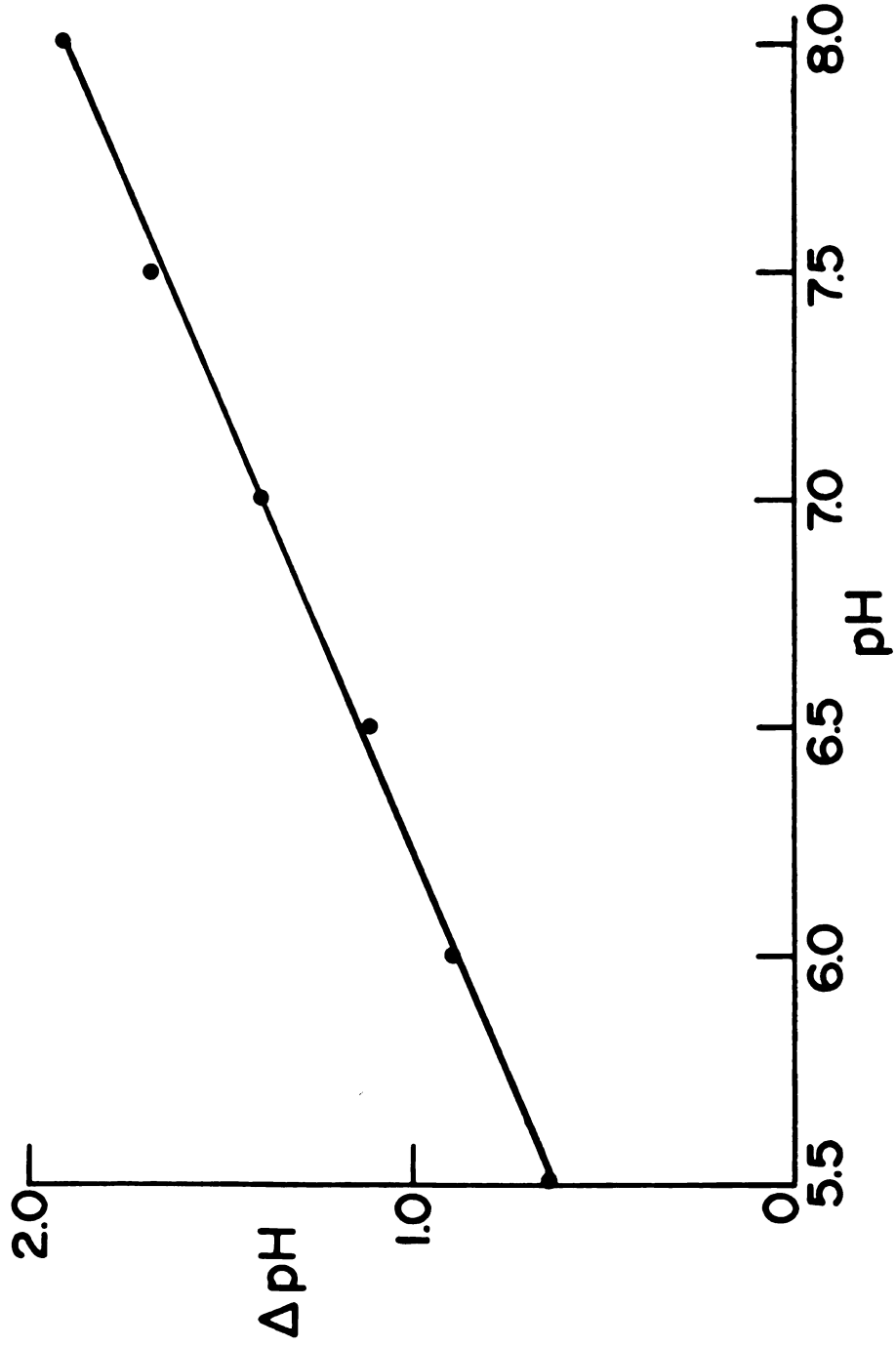
2.0
1.0
0
ΔpH
5.5
6.0
6.5
7.0
7.5
8.0
pH

with increasing pH can be qualitatively explained by the model developed in Section I. As Figure 9 illustrates, an uncoupling agent with a pKa that falls in or below the experimental pH range gives rise to a variation in ΔpH with pH. At least two species with pKa values in this range, TRIS with a pKa = 8.08 and the buffer (MES with a pKa = 6.1, HEPES with a pKa = 7.5 or TRICINE with a pKa = 8.1) are present in the chloroplast suspension and could be acting as weak, pH dependent uncoupling agents. This could also explain the difference observed between the two different chloroplast preparations. The difference in pH dependence may reflect the more efficient washing of one sample to remove TRIS buffer from the suspension. This experimental difference could lead to different levels of uncoupling efficiency and consequently to different pH dependencies.

A second model to explain the pH dependence of the kinetics involves the postulation of a net negative charge on the inside of the thylakoid membrane, an idea which could also help to explain the large difference in the magnitudes of k_1 and k_2. The magnitude of k_1, which is associated with the reduction of $Z^{+\cdot}$ by neutral ascorbate, if twenty times greater than that of k_2, associated with the reduction of $Z^{+\cdot}$ by the ascorbate anion. This suggests that $Z^{+\cdot}$ may be more accessible to the neutral form of the reducing agent than to its anion. This could be explained by a net negative charge on the internal membrane surface. Support for the presence of this surface charge comes from the electrophoretic experiments conducted by Nakatani _et al_. (1978) which demonstrate the presence of a net negative charge on the exterior of the thylakoid membrane. They studied the effect of pH on the mobility of the thylakoid membrane when placed in a

conducting solution in the presence of an electrical field. When the suspension pH is greater than 4.3, the thylakoids move toward the anode, demonstrating that they carry a net negative charge. Below pH values of 4.3, the direction of electrophoretic migration is reversed. These results were interpreted to indicate that there exist, on the exterior surface of the thylakoid, groups with a pKa of about 4.3. If the internal surface of the thylakoid carries a similar charge at neutral pH, the following scheme might explain the pH dependence of signal II_f decay. As the pH of the suspension medium, and therefore of the thylakoid interior, decreases, an increasing fraction of the surface negative charges, possibly arising from carboxyl groups or pigment-protein complexes of the antenna chlorophyll (Nakatani *et al.*, 1978), would protonate, leading to a decrease in the surface charge. This would result in an effective increase in the magnitude of k_2, the rate constant assocated with the anionic reducing agent, since the ascorbate anion would be less strongly repelled by the membrane as the net negative charge on it surface was decreased. Good fits to the experimental data are obtained for values of k_2 which range between about 2200 $\underline{M}^{-1}$ s^{-1} at pH = 5.5 to 800 $\underline{M}^{-1}$ s^{-1} at pH = 8.5. Further experiments by Nakatani *et al.* (1978), however, suggest that this explanation of the pH dependence of signal II_f decay may be unlikely. Between pH values of 6.0 and 10.0, the rate of electrophoretic migration of the thylakoid is found to be independent of pH, indicating no change in the magnitude of the exterior surface negative charge in this pH range. However, the experiments of Itoh (1978) on ferricyanide reduction demonstrate that the negative charge on the exterior of the thylakoids

can at least be masked, if not neutralized, by variation of the suspension pH, as discussed in Section I-D. All of these experiments reflect the nature of the exterior surface of the thylakoid membrane and whether the interior exhibits a similar net charge or will behave analogously to variations in pH remains to be tested.

Experiments are planned to test both of these models. A study will be made of signal II_f decay kinetics in the presence and absence of ammonium ion. If the addition of this known uncoupling agent is found to depress the pH dependence, presumably through the dissipation of the ΔpH across the membrane, support would be gained for the first model. The second model will be tested by studying the pH dependence of signal II_f decay upon addition of nigericin and variation of salt concentration. Nigericin selectively permits the incorporation of potassium ions into the thylakoid compartment (Shavit et al., 1968). A variation in the pH dependence with potassium ion concentration could demonstrate the shielding of negative surface charges by the cation, with a concomitant increase in the magnitude of k_2.

An additional set of experiments, those involving hydroquinone as the exogenous electron donor, substantiates the placement of $Z^{+\cdot}$ in an environment more easily accessible to neutral than to charged species. Hydroquinone, with a pKa of 10.34, was selected as an electron donor because over the experimental pH range, it exists almost exclusively in its neutral form. The used of relatively low concentrations of hydroquinone, 10^{-5} M, necessitated the addition of ascorbate to reduce the hydroquinone oxidized by $Z^{+\cdot}$. The use

of hydroquinone substantially decreases the half-time of signal II_f decay as illustrated in Figure 18. The decay of Signal II_f in the presence of hydroquinone follows pseudo-first order kinetics, which allows the computation of a hydroquinone rate constant, k_{HQ}, from the relationship $k_{obs} = k_{HQ}$ [HQ]. At pH = 5.5, the calculated k_{HQ} = 9.59×10^5 $\underline{M}^{-1}$ s^{-1}. As a comparison of the relative efficiency of neutral ascorbate and hydroquinone as reductants of $Z^{+\cdot}$, this k_{HQ} can be compared to k_1 from the ascorbate case at pH = 5.5, when the k_1 term is dominant and the kinetics reduce to $k_{obs} = k_1$ [HAsc]. The value of k_1 under these conditions is about 7.75×10^4 $\underline{M}^{-1}$ s^{-1}. A comparison of these rate constants shows that hydroquinone is about ten times more efficient than ascorbate in reducing $Z^{+\cdot}$. This may indicate the situation of $Z^{+\cdot}$ in a highly non-polar environment but additional work is required before such an assignment may be made.

The studies described have provided information about the role of the thylakoid membrane in the chemical reactions of plant photosynthesis. The results and the models derived from them contribute to the understanding of the function of the membrane in photosynthetic oxygen evolution and emphasize the importance of this role.

BIBLIOGRAPHY

BIBLIOGRAPHY

Babcock, G. and Sauer, K. (1973) Biochim. Biophys. Acta, 325, 483.

Babcock, G. and Sauer, K. (1975) Biochim. Biophys. Acta, 376, 315.

Beinert, H. and Kok, B. (1964) Biochim. Biophys. Acta, 88, 278.

Blankenship, R.E. and Sauer, K. (1974) Biochim. Biophys. Acta, 357, 252.

Blankenship, R.E., Babcock, G., Warden, J. and Sauer, K. (1975) FEBS Letters, 51, 287.

Briantais, J-M., Vernotte, C., Lavergne, J. and Arntzen, C.J. (1977) Biochim. Biophys. Acta, 461, 61.

Butler, W.L., Visser, J.W.M., and Simons, H.L. (1973) Biochim. Biophys. Acta, 325, 539.

Cheniae, G.M. and Martin, I.F. (1966) in Energy Conversion by the Photosynthetic Apparatus, Brookhaven Symp. Biol., 19, 406.

Crofts, A.R. (1976) J. Biol. Chem., 25, 3352.

Delrieu, M.J. (1976) Biochim. Biophys. Acta, 440, 176.

Duysens, L.N.M. and Sweers, H.E. (1963) in Studies in Microalgae and Photosynthetic Bacteria (Japanese Soc. Plant Physiologists, ed.) pp. 353-372, University of Tokyo Press, Tokyo.

Emerson, K. and Arnold, W. (1932) J. Gen. Physiol., 15, 391.

Floyd, R.A., Chance, B. and Devault, D. (1971) Biochim. Biophys. Acta, 226, 103.

Good, N.E. (1960) Biochim. Biophys. Acta, 40, 502.

Hanstein, W.G. (1976) Biochim. Biophys. Acta, 456, 129.

Heise, J.J. and Treharne, R.W. (1964) in Developments in Applied Spectroscopy (Forrette, J.E. and Lanterman, E., eds.) p. 340, Plenum Press, New York.

Hoaglund, D.K. and Brayer, T.C. (1936) Plant Phys., 11.

Holt, A.S. and French, C.S. (1948) Archiv. Biochem., 19, 368.

Itoh, S. (1978) Plant and Cell Physiol., 19 (1), 149.

Jagendorf, A.T. and Neumann, J. (166) J. Biol. Chem., 240, 3210.

Joliot, P., Barbieri, G. and Chabaud, R. (1969) Photochem. Photobiol., 10, 309.

Joliot, P., Bouges, B. and Barbieri, G. (1971) Photochem. Photobiol., 14, 287.

Junge, W. and Witt, H.T. (1968) Z. Naturforsch., 23b, 244.

Kohl, D.H. (1972) in Biological Applications of ESR (Schwartz, H.M. et al., eds.) p. 213, John Wiley and Sons, New York

Kok, B. and Cheniae, G.M. (1966) in Current Topics in Bioenergetics (Sanadi, D.R., ed.) Vol. 1, pp 1-47, Academic Press, New York and London.

Kok, B., Forbush, B. and McGloin, M. (1970) Photochem. Photobiol., 11, 45.

Lavorel, J. (1975) in Bioenergetics of Photosynthesis (Govindjee, ed.) pp 225-314, Academic Press, New York.

Mitchell, P. (1966) Biol. Rev., 41, 445.

Renger, G., Glaser, M. and Buchwald, H.E. (1977) Biochim. Biophys. Acta, 461, 392.

Rottenberg, H. and Grunwald, T. (1972) Eur. J. Biochem., 25, 71.

Sauer, K. (1978) Acc. Chem. Res., 11, 257.

Schuldiner, S., Rottenberg, H. and Avron, M. (1972) Eur. J. Biochem., 25, 64.

Shavit, N., Dilley, R.A. and San Pietro, A. (1968) Biochem., 7, 2356.

Siefermann-Harms, D. (1978) Biochim. Biophys. Acta, 504, 265.

Sun, A.S.K. and Sauer, K. (1971) Biochim. Biophys. Acta, 234, 483.

Van Best, J.A. (1977) Dissertation, University of Leiden.

Van Best, J.A. and Mathis, P. (1978) Biochim. Biophys. Acta, 503, 178.

Van Gorkom, H.J., Tamminga, J.J., Haverman, T. and Van der Linden, I.K. (1974) Biochim. Biophys. Acta, 347, 417.

Warden, J.T., Blankenship, R.E. and Sauer, K. (1976) Biochim. Biophys. Acta, 423, 462.

Weaver, E.C. (1968) Ann. Rev. Plant Physiol., 19, 283.

Yamashita, T. and Butler, W.L. (1969) Plant Phys., 44, 435.